Environmental Science Processes & Impacts

The Importance of Charge-Transfer Interactions in Determining Chromophoric Dissolved Organic Matter (CDOM) Optical and Photochemical Properties

Journal:	*Environmental Science: Processes & Impacts*
Manuscript ID:	EM-CRV-10-2013-000573.R2
Article Type:	Critical Review
Date Submitted by the Author:	23-Jan-2014
Complete List of Authors:	Sharpless, Charles; University of Mary Washington, Department of Chemistry Blough, Neil ; University of Maryland, Chemistry & Biochemistry

Environmental Impact Statement

The use of spectroscopic techniques to monitor chromophoric dissolved organic matter (CDOM) transport and fate has risen steadily, buoyed by relationships between CDOM source and optical properties. Research also shows that CDOM photochemical reactivity depends strongly on its optical properties. While these empirical relationships between CDOM source, optical, and photochemical properties represent potentially useful tools for studying and predicting rates and processes of CDOM transformation and photochemical reactions, their underlying physical basis is not firmly established. Such knowledge would improve interpretations based the empirical relationships and provide a foundation on which to refine and expand them. This review summarizes current understanding of how CDOM composition controls its optical and photochemical properties and indicates areas for further research.

The Importance of Charge-Transfer Interactions in Determining Chromophoric Dissolved Organic Matter (CDOM) Optical and Photochemical Properties

Authors

Charles M. Sharpless[a,*], Neil V. Blough[b,*]

[a] Department of Chemistry, University of Mary Washington, Fredericksburg, VA 22401 USA

[b] Department of Chemistry, University of Maryland, College Park, MD 20742 USA

* Corresponding author

csharple@umw.edu, (phone) +001 540.654.1405, (fax) +001 540.654.1405

neilb@umd.edu, (phone): +001 301.405.0051, (fax) +001 301.314.9121

Abstract

Absorption of sunlight by chromophoric dissolved natural organic matter (CDOM) is environmentally significant because it controls photic zone depth and causes photochemistry that affects elemental cycling and contaminant fate. Both the optics (absorbance and fluorescence) and photochemistry of CDOM display unusual properties that cannot easily be ascribed to a superposition of individual chromophores. These include (i) broad, unstructured absorbance that decreases monotonically well into the visible and near IR, (ii) fluorescence emission spectra that all fall into a single envelope regardless of the excitation wavelength, and (iii) photobleaching and photochemical quantum yields that decrease monotonically with increasing wavelength. In contrast to a simple superposition model, these phenomena and others can be reasonably well explained by a physical model in which charge-transfer interactions between electron donating and accepting chromophores within the CDOM control the optical and photophysical properties. This review summarizes current understanding of the processes underlying CDOM photophysics and photochemistry as well as their physical basis.

1. Introduction

Chromophoric dissolved organic matter (CDOM) is the light-absorbing fraction of dissolved organic matter. It can originate from both aquatic microbial sources and terrestrial sources such as lignin that have degraded and dissolved; for purposes of this review, we refer to these materials as microbial and terrestrial, respectively. Absorption of sunlight by CDOM controls photic zone depths (*1-6*) and initiates a variety of photochemical reactions that convert CDOM to inorganic carbon (*6-14*) and biologically-available, low molecular weight compounds (*5,15-18*), affect trace-metal redox speciation (*7,19-21*), influence the fate of aquatic

contaminants (*22-29*), and in some instances can contribute significantly to aquatic oxygen demand (*30-33*). The optical and photochemical properties of CDOM vary with season, CDOM source, and water chemistry (*2,34-41*). An outstanding challenge for environmental scientists is to understand these variations and predict their impact on elemental cycling and the fate of anthropogenic compounds.

The color of CDOM comes predominantly from humic substances (HS), which comprise humic acids (HA, soluble above pH 2) and fulvic acids (FA, soluble at all pH values) (*42*). A battery of analytical techniques has been employed to gain structural information about CDOM including pyrolysis-mass spectrometry (*43-45*), high- and ultrahigh-resolution mass spectroscopy (*46-50*), ^{13}C nuclear magnetic resonance spectroscopy (*48,51,52*), electron spin resonance spectroscopy (*53,54*), acidimetric titrations (*55-57*), and electrochemistry (*58,59*). These studies indicate that CDOM contains a variety of structures including carboxylic acids and carboxyl-rich alicyclic molecules, substituted phenols, ketones, aldehydes, quinones, carbohydrates, saturated and unsaturated hydrocarbons, and nitrogenous material (*60,61*).

All of the evidence suggests that CDOM absorption and photochemistry originates from aromatic chromophores. However, the complexity of the mixture makes it exceedingly difficult to identify the precise structures that produce these phenomena. Furthermore, CDOM exhibits unusual optical and photochemical properties that are inconsistent with the behavior of individual chromophores or even the behavior of a collection of independent chromophores. This review summarizes these properties and current understanding of their molecular basis. We advance the idea that much of the observed behavior can be explained by electronic interactions between chromophores, which produce an array of photophysical and photochemical reaction channels. We further argue that the relative importance of each channel varies with CDOM

source and environmental conditions due to varying abundance of electron donating and accepting groups and the effects of solution chemistry on excited-state energies. In Section 2, the optical properties are reviewed, and an electronic interaction model is introduced. Section 3 covers CDOM photochemistry, the implications of the electronic interaction model for the photochemistry, and concludes with a brief review of correlations between CDOM optical and photochemical properties.

2. CDOM Optical Properties

The optical absorption and emission properties of CDOM in both fresh and marine waters have been investigated extensively over the last several decades. Much of this past work has been summarized in a series of prior review articles to which interested readers are referred for more details (*2,34,35,62-65*).

2.1 Absorption

CDOM absorption in most natural waters decreases monotonically with increasing wavelength in an approximately exponential fashion, usually with no readily discernible absorption bands (Fig. 1). How quickly the absorption decreases with increasing wavelength varies geographically and seasonally, presumably due to variations in source as well as through biological and (photo)chemical processing (*2,34,35,62-65*). To quantify these variations, spectra are often fit to an exponential equation, with the exponent of these fits, the spectral slope parameter, S, providing an indication of how rapidly absorption decreases (*2,35,62-65*); higher values of S indicate a more rapid decline and a lower absorption contribution in the visible wavelengths. Other empirical indices of this decline include the E2/E3 and E4/E6 ratios; the E2/E3 ratio represents the ratio of absorption at 254 nm to that at 365 nm (*66*) while the E4/E6 ratio represents the ratio at 465 nm to that at 665 nm (*62*). More recently, workers have used fits

to other equations (*67*) or exponential fitting over more limited wavelength regimes (*68-72*) in order to characterize the absorption spectra in more detail. The aim of this characterization is ultimately to relate the differences in spectral line-shape to variations in source and changes in the structural properties of the CDOM produced by chemical and biological processing.

Based on these types of studies, numerous workers have found that S usually increases with decreasing molecular size (*2,62,66,73-76*). Photobleaching of CDOM in surface waters under solar irradiation also usually increases S and E2/E3 (Fig. 1) (*2,63,65,68,75,77-80*) or ratios of S over differing spectral regions (*68,80*), suggesting that photochemical reactions increase S by converting high molecular weight species to lower molecular weight species (*68,81*). The highest values of S are generally observed for offshore marine surface waters (>0.020 nm^{-1}), with intermediate values observed for estuarine, coastal and freshwaters (~0.014 to 0.018 nm^{-1}), and the lowest values for soil HS (~0.010 to 0.014 nm^{-1}) (*2,34,35,62-65*). How much S varies in aquatic systems due to differences in the source of CDOM as opposed to (photo)chemical and/or biological processing of a given source material remains highly uncertain (*2,35,65,80,82*) and is an active area of research. The possible structural basis of variations in S and how they may be related to photochemical processes are discussed further below.

Specific absorption coefficients (*62*) and SUVA (*66,83,84*), obtained by normalizing absorption to organic carbon concentration, have also been used to characterize HS and CDOM and provide a measure of how strongly these materials absorb light on a mass-carbon basis. For isolated HS, specific absorption coefficients (and SUVA) have been reported to increase with increasing molecular weight and with percent aromaticity (*66,83,84*) and be larger for HA than FA (*62,83*). Because not all carbon is absorbing, however, these parameters are far less useful than S for characterizing CDOM in natural waters; one cannot distinguish between a small

amount of highly absorbing material embedded in a non-absorbing high-carbon background and a larger amount of more weakly absorbing material embedded in a non-absorbing low-carbon background. Furthermore, absorption by high levels of inorganic species such as nitrite and nitrate as well as metal complexes can sometimes confound the interpretation of these parameters (*83*).

2.2 Fluorescence

Fluorescence emission spectra acquired for the "humic-like" component of CDOM are very broad and unstructured, exhibiting emission maxima that red-shift continuously with increasing excitation wavelength (Fig. 2) (*74,82,85,86*). Fluorescence quantum yields are very low, on the order of 0.1-2% depending on source (*74,82,87,88*), and decrease at both shorter and longer wavelengths from the maximum value, which is usually found with excitation between 350 and 400 nm (*74,82,87,88*). Consistent with the quantum yields, fluorescence lifetimes are also very short, predominantly sub-nanosecond, and decrease monotonically at longer wavelengths on the red edge of the visible emission (*74,89*), as well as on the blue edge when shorter-wavelength excitation is employed (*89,90*). Additionally, substantial Stokes shifts, on the order of 150-200 nm, are usually observed upon short wavelength excitation (≤300 nm) (Fig. 2) (*82,91-93*).

Fluorescence quantum yields and lifetimes usually increase with decreasing molecular size (*74,88,94*), indicative of intramolecular quenching interactions in the higher molecular weight material (*74*). In stratified surface waters where photobleaching can take place, and in laboratory photobleaching studies, emission maxima are shifted to shorter wavelengths (*74,80,82,95,96*). Reduction of aquatic samples with sodium borohydride also produces substantially-enhanced, blue-shifted emission (Fig. 2) along with a preferential loss of absorption

128 in the visible (Fig. 1), leading to ~3- to 6-fold increases in the fluorescence quantum yields on
129 the blue edge of the emission (*82,97*). Along with the unstructured, broad-band absorption, these
130 results point to the presence of numerous absorbing and emitting centers, some of which may be
131 due to a number of electronically-isolated chromophores while others are explainable by
132 chromophore-chromophore interactions in both the ground and excited state as discussed in
133 Section 2.3 below.

134 In addition to the "humic-like" component, distinct bands have been observed upon
135 excitation below approximately 290 nm that have emission maxima consistent with those of
136 tyrosine or other phenols (302 nm) and tryptophan (354 nm) (*2,65,91*). Other bands have been
137 observed that have yet to be related to possible structures (*65,82*). To our knowledge, evidence
138 for distinct emission bands has only been found for species absorbing and emitting in the
139 ultraviolet; as noted above, the continuous red-shift of the emission maxima in the visible with
140 increasing excitation wavelength, along with the monotonically-decreasing fluorescence
141 quantum yields (*74,82,87*) and fluorescence lifetimes (*74,89*) imply the presence of a near-
142 continuum of emitting species or states (*62,74,85,89*).

143 Over the past 10 years, excitation-emission matrix spectroscopy (EEMS, Figs. 2c and 2d)
144 combined with Parallel Factor Analysis (PARAFAC) has been employed increasingly to fit the
145 fluorescence spectra of CDOM to a varying number of components having distinct excitation
146 and emission spectra (*98,99*). In earlier studies, these components were often interpreted to be
147 distinct fluorophores (*92,100*), which in some cases led to incorrect assignments of components
148 to specific structures (*101-103*). A major assumption of PARAFAC is that all species giving rise
149 to emission absorb and emit light independently of one another, or in other words are
150 electronically-isolated (*98,99*). Although reasonable for the distinct emission bands often

observed in the ultraviolet, this assumption is highly questionable for the "humic-like" fluorescence observed in the visible (see above). The complex spectral dependence of the steady-state and time resolved emission cannot be easily reconciled with a simple superposition of a small number of independently-absorbing and emitting PARAFAC components (*74,85*). The central question is whether these PARAFAC components reveal anything about the underlying structures producing the "humic-like" emission. While EEMS combined with PARAFAC can be a very useful empirical tool for characterizing very large fluorescence data sets to examine how the fitted components might vary geographically and seasonally (*104-106*), in our view the use of this approach alone is unlikely to provide much insight into the structures producing the "humic-like" emission. This information is essential not only for refining spectral approaches to tracking CDOM source, but also for understanding how these structures are involved in photochemical reactions and how CDOM may be modified by biological and (photo)chemical processes.

2.3 Structural Basis of Absorption/Emission Spectra

In principle, two distinct models might explain the optical properties of CDOM, namely a superposition model or an electronic interaction model. PARAFAC provides an example of a superposition model in which all chromophores within the mixture are assumed to absorb and emit light independently. The observed spectra thus represent a simple sum of the individual spectra of the participating chromophores (see also ref. (*107*)). This model does not account for possible electronic interactions between chromophores that could lead to altered emission properties through, for example, energy or electron transfer, nor to broadened and new electronic transitions produced, for example, through chromophore stacking and charge transfer interactions (electronic interaction model, (*74,85*)). Because of chromophore-chromophore

interactions, the observed spectra will no longer be a simple sum of the spectra of the individual (electronically-isolated) chromophores. Although evidence against a superposition model continues to accumulate (see below), PARAFAC fitting is still employed widely to describe the emission properties of CDOM.

Any optical model of CDOM must account for a number of rather unusual photophysical and photochemical properties. These include: (1) unstructured, broad-band absorption that extends to low energies well into the visible region (Fig. 1) (*2,44,62,63,65,67,73,85*); (2) preferential decreases in visible absorption (increases in S) with photobleaching (Fig. 1) (*68,78-80*) and with decreasing molecular size (*66,73,74*) (Fig. 1); (3) continuously red-shifting emission maxima as excitation wavelengths increase (Fig. 2) combined with low and monotonically decreasing fluorescence quantum yields and lifetimes on both the blue and red edges of the emission (*74,85,87,89,90*); (4) preferential loss of visible absorption and enhanced, blue shifted fluorescence with borohydride reduction (Fig. 2) (*82,97,108-110*); (5) photochemical and photobleaching quantum efficiencies that decrease rapidly with increasing wavelength and that are very small or indistinguishable from zero at visible wavelengths (Fig. 3) (*12,14,18,38,77-79,111-113*).

A superposition model could only explain the low energy transitions in the visible as resulting from a superposition of either highly-extended aromatic or heteroaromatic structures, or highly-extended conjugated structures. There are, however, a number of problems with this explanation. First, NMR, mass spectrometry and fluorescence spectroscopy provide little evidence for the widespread occurrence of these types of structures in CDOM. Indeed, results from ultra-high resolution mass spectrometry and fluorescence spectroscopy suggest a primarily lignin-based origin for terrestrial HS and inland as well as coastal CDOM (*74,109,110,114-118*).

Moreover, numerous studies have found excellent correlations between CDOM absorption and lignin phenol content in natural waters (*74,119-123*) and following photobleaching (*122*). Because the aromaticity of lignin primarily derives from single aromatic rings that are electronically isolated by o-ether linkages, long-wavelength visible absorption would not be anticipated for lignins *a priori*. While possible oxidation products of lignins such as quinones are known to absorb in the visible (*97*), their molar absorptivities (*97*) and concentrations (*58,97*) are far too low in most instances to contribute significantly; additionally, a rather unbelievably distinct distribution of quinones would be required to explain simultaneously the spectral dependence of the visible absorption and the redox properties (*58,97*). Thus, a simple superposition of the absorption and emission by lignin oxidation products in the visible also appears incompatible with the evidence (*97,102*).

Second, owing to the continuously red-shifting emission maxima and monotonically decreasing fluorescence quantum yields and lifetimes observed at visible wavelengths, a superposition model would require uniquely that the compounds absorbing at these increasingly lower energies (more highly extended aromatic or conjugated structures) exhibit systematically smaller fluorescence quantum yields and lifetimes. Because no unique relationship exists between the first excited singlet-state energy of aromatic or conjugated compounds and their fluorescence quantum yields and lifetimes, this observation is also incompatible with a superposition model. For example, chlorophylls and porphyrins absorb at very low energies in the visible but can have very high fluorescence quantum yields.

Third, and as a corollary to the preceding point, the rapid decrease with increasing wavelength of the apparent quantum efficiencies for reactive intermediate production (Fig. 3) and photobleaching (*77*) is also incompatible with a superposition model: there is no

fundamental reason to expect that distinct chromophores absorbing at increasingly lower energies in the visible will have systematically lower quantum efficiencies for these processes (or for fluorescence). For example, porphyrins, chlorins, Rose Bengal and many condensed polycyclic aromatic hydrocarbons (eg., perylene), to name just a few compounds and compound classes, all absorb at wavelengths well into the visible but exhibit high and variable yields of singlet dioxygen production. Indeed, within the superposition model the exceedingly low or negligible quantum efficiencies for reactive intermediate production and photobleaching observed with visible excitation would require that the individual compounds absorbing at these longer wavelengths neither undergo direct photochemistry nor act as photochemical sensitizers, rather unusual behavior for most aromatic compounds.

In contrast to the superposition model, an electronic interaction model can largely account for the optical and photochemical properties of CDOM. This model proposes that the optical properties of terrestrial CDOM arise in part through electronic interactions among chromophores within partially-oxidized oligomeric/polymeric hydroxy-/methoxy aromatics such as lignin, tannins, and polyphenols (*74,85,89,109,110,116*). Within the electronic interaction model, short-range, charge transfer (CT) interactions between electron-rich donors and electron-deficient acceptors (*124,125*), formed through partial oxidation of lignin (or other polyphenolic precursors), are of primary importance, as they can provide an explanation for the long-wavelength, near-UV and visible absorption and emission properties of CDOM. These interactions are capable of producing new, lower energy, optical CT transitions (*85,124,126*) arising from short-range contacts between hydroxy-/methoxy-aromatic electron donors and carbonyl-containing electron acceptors (*74,85,89,127,128*). The CT model thus proposes that the long-wavelength absorption and emission in the near-UV and visible results primarily from

intramolecular CT complexes between hydroxy-/methoxy-aromatic electron donors and carbonyl-containing electron acceptors formed through the partial oxidation of lignin precursors (*74,85,89,127,128*). Within lignin, electron donors could include phenols and/or methoxylated phenols, while acceptors could include quinones and/or (aromatic) ketones/aldehydes.

According to the CT model, the increase in S with decreasing size can be attributed to the smaller number and variety of CT contacts statistically possible within the smaller molecules of the size ensemble (*74,85*). The increase in S with photobleaching (Fig. 1) and with chemical oxidation (*68,80,129,130,131*) can be explained by both a reduction in the average size of the ensemble as well as by the destruction of electron donors and acceptors contributing to the CT transitions. In fact, the observation that photobleaching and chemical oxidation simultaneously decrease $SUVA_{254}$ while increasing S suggests that destruction of electron donors and acceptors is central to the loss of CT absorbance (*68,80,129,130,131*).

The spectral slope parameter, S, has also been observed to decrease with increasing pH (*39,56,132*), particularly over the pH range where phenols are deprotonated (*56,132*). While deprotonation of simple phenols would be expected to shift the absorption to the red by 15-20 nm (*133*), these shifts in absorption would be restricted to the UV. In contrast, substantial increases in absorption are also observed across the visible (*56,132*). Because phenolate anions are much better electron donors than the neutral phenols (*134*), a reasonable explanation for this increase in visible absorption is that CT interactions are enhanced under alkaline conditions.

In terms of the fluorescence, the CT model explains the continuously red-shifting emission maxima and the very small and monotonically decreasing fluorescence quantum yields and lifetimes as due to charge recombination luminescence from an ensemble of low-energy CT states populated by near-UV and visible absorption. Emission red-shifts that occur with

increasing pH (*86*) suggest an increased influence of CT states occurs upon dissociation of acidic aromatic donor groups. The decrease in quantum yields and lifetimes with decreasing energy (increasing emission wavelength) can be attributed to an energy gap dependence; at successively lower CT energies, the rate of non-radiative relaxation increases relative to the radiative rate thus leading to lower fluorescence quantum yields and shorter lifetimes (*124*). Moreover, the lack of discernable photochemistry in most of the visible region (Fig. 3) is fully consistent with very rapid relaxation of these states through charge recombination. Finally, the large Stoke's shifts with short wavelength excitation produce emission spectra that reproduce many features obtained with longer wavelength excitation (Fig. 2) (*82,91-93*). This suggests that lower energy CT states similar to those obtained by direct CT absorption are populated from higher-energy excited state donors via energy (or electron) transfer (*74,124*).

Another prediction of the CT model is that the removal of either the donor or acceptor moieties will eliminate CT interactions and thus reduce the long-wavelength absorption and fluorescence emission. Consistent with this prediction, partial photobleaching causes blue shifts in emission maxima (*80,95*), which can be explained as enhanced emission from higher energy (donor) species as decreasing CDOM molecular size eliminates quenching due to CT interactions (*74*). Further, employing sodium borohydride as a selective reductant of carbonyl-containing electron acceptors, namely (aromatic) ketones/ aldehydes and quinones, it has been demonstrated that reduction of microbial and terrestrial HS, a commercial lignin, C18 extracts from the MAB shelf and the Equatorial Atlantic, as well as natural waters alone, produces preferential loss of visible absorption (Fig. 1) and substantially enhanced, blue-shifted fluorescence emission (Fig. 2) (*82,97,108*). Importantly, these observations preclude major contributions to visible absorbance from compounds that do not undergo reduction with borohydride. This includes all

289 extended aromatic structures or highly conjugated structures, unless they contain a borohydride-
290 reducible carbonyl moiety in resonance with the aromatic or conjugated structure. The
291 enhanced, blue-shifted emission observed following borohydride reduction does not appear to
292 arise from the reduced products, but instead likely arises from donor species that are no longer
293 quenched after removal of CT interactions (*97*).

294 While quinones were originally anticipated to play a major role as electron acceptors in
295 CT transitions (*85*), currently available evidence suggests that (aromatic) ketone/aldehyde
296 acceptors are far more important determinants of CDOM optical properties (*97,109,116*).
297 Structural considerations suggest that substituted phenols are important high energy donor
298 species (*74,109,110,114-118*). These structural elements thus form the basis for the CT model of
299 CDOM optical properties. The optical properties themselves imply a large degree of rapid
300 photophysical relaxation via electron transfer interactions of these chromophores. Nonetheless, a
301 small fraction of excited states produce environmentally relevant photochemistry, many aspects
302 of which find logical explanations in the CT model. This topic is the subject of the following
303 section.

304 *3. Mechanistic Aspects of CDOM Photochemistry*

305 It has been clear since the 1980's that CDOM photochemistry can be an important
306 determinant of surface water chemistry. Seminal work during that era demonstrated CDOM as a
307 photochemical source of singlet oxygen ($^1O_2$) (*135,136*), superoxide (O_2^-) and its dismutation
308 product hydrogen peroxide (H_2O_2) (*137,138*), aqueous electron (e^-(aq)) (*139,140*), and organic
309 radicals (*141,142*). It has since been shown that CDOM photochemistry also produces hydroxyl
310 radical (•OH) (*143,144*) and excited triplet states of CDOM (^{3}CDOM*) as important
311 photooxidants (*22,145*). All of these species can collectively be referred to as photochemically

produced reactive intermediates (PPRIs). Interested readers can find methods for detecting and studying PPRIs reviewed elsewhere (*146-148*). Absorption of light also photobleaches CDOM (*149*) and eventually leads to its photomineralization (*40*); this latter process is potentially significant to the global carbon budget, though a precise assessment of its magnitude has been difficult (*8*).

Figure 4 illustrates a model to explain the various reactions. Central to this scheme is the lack of photochemistry occurring via CT absorbance (reaction 2) and competitive decay of singlet excited state CDOM (^{1}CDOM*) into either ^{3}CDOM* (reaction 6) or charge-separated species formed by donor-acceptor electron transfer ($CDOM^{+\bullet/-\bullet}$) (reaction 7). Much of the following discussion focuses on apparent quantum yields (i.e., the moles of PPRI produced per mole of photons absorbed) because that parameter indicates the kinetic efficiency of individual reaction channels. The qualifying term "apparent" indicates that the quantum yields in question are not primary but result from complex reaction mechanisms. For brevity, the following discussion employs the term "quantum yields" with the implicit understanding that this refers to apparent quantum yields.

3.1 Photooxidation

Photochemical oxidation of CDOM is an important albeit poorly constrained part of the global carbon cycle (*8,9*). The initial stages of the process are characterized by rapid loss of chromophores and photobleaching. Various studies have shown that phenols and other aromatic components are particularly susceptible to photooxidation and are destroyed on similar time scales as the absorbance loss (*122,123,150-153*). As noted above, photobleaching causes a more rapid loss of visible than UV absorbance, which concomitantly increases S and the E2/E3 ratio (*68,75,77-79,149*).

It is tempting to suspect that the mechanisms of photobleaching and photooxidation involve reactive oxygen species (ROS). Indeed, in cases where very high •OH photoproduction can occur via nitrate or nitrite photolysis (*143*) or photofenton reactions (e.g., low pH, Fe(III)-rich waters), this ROS may play a small role in photomineralization (*16*). However, there is little evidence that ROS sensitized by CDOM itself (e.g., $^1O_2$ and •OH) play a role in photooxidation. Support for such an idea is indirect, for example similar wavelength dependencies of ROS quantum yields (*147*) (Fig. 3), photobleaching quantum yields (*107,154,155*), and dissolved inorganic carbon quantum yields, which range from $5x10^{-4}$ to $5x10^{-3}$ at approximately 350 nm (*40,154,156*) (Fig. 3). However, there is good evidence against the involvement of ROS produced by CDOM. A self-sensitized reaction would occur with 2nd order kinetics, but photobleaching commonly follows 1st order or multi-phasic kinetics. Furthermore, experiments designed to test for the involvement of •OH and $^1O_2$ in CDOM photooxidation (*157,158*) and photobleaching (*32,159,160*) demonstrate at most a small effect of these species. Direct oxidation of ^{3}CDOM* with O_2 (*160*) does not appear plausible because current evidence indicates that ^{3}CDOM* is not a precursor to H_2O_2 (*110*). Alternatively, the magnitude of dissolved inorganic carbon (DIC) quantum yields are roughly consistent with the extent of e^- transfer indicated by O_2^-/H_2O_2 quantum yields (see below), and a link between H_2O_2 and DIC production (oxidation) is suggested by the fact that both H_2O_2 and DIC quantum yields increase with pH (*39,156*). Thus, the suspected H_2O_2 precursor, $CDOM^{+\bullet/-\bullet}$, could be an important intermediate in photooxidation. Further research is needed to ascertain this.

3.2 Formation and Environmental Significance of Specific PPRIs

3.2.a. Aqueous Electron

Photoionization of CDOM to produce $e^-(aq)$ has been demonstrated at excitation wavelengths from 250 to 400 nm using both steady-state and laser flash photolysis techniques (*37,111,140,161-163*). The source of $e^-(aq)$ is undoubtedly aromatic groups; phenols and their derivatives are well-known to eject $e^-(aq)$ from excited singlet states (*125*), and this behavior is observed with aromatic carboxylic acids (*164*) and aromatic amino acids (*165*). Other evidence suggesting the involvement of phenols and aromatic carboxylic acids is that $e^-(aq)$ production increases at high pH (*140*), and synthetic humic acid produced by phenol polymerization generates $e^-(aq)$ but not $^1O_2$ (*162*). In addition, $e^-(aq)$ quantum yields (Φ_{e^-}) increase rapidly with decreasing wavelength (Fig. 3), becoming approximately 100x larger at 254 nm than at 350 nm (*111,162*), consistent with the hypothesis that short-wavelength irradiation directly excites electron donating chromophores such as phenols.

Early results from laser flash photolysis studies found Φ_{e^-} to be approximately $5x10^{-3}$ at 355 nm (*161*). However, recent work has shown that this value is much too large due to multi-photon excitation (*37,111*). It is now established that Φ_{e^-} varies from approximately 10^{-4} to 10^{-5} over the wavelength range 300 to 400 nm (*37,111*). Given such low efficiencies and the fact that other components of natural waters such as tryptophan (free or in combined form) generate $e^-(aq)$ (*111*), it is unlikely that CDOM-derived $e^-(aq)$ has a significant environmental impact. However, it may play a role in the photodegradation of hydrophobic chlorinated compounds that partition into the CDOM microenvironment (*23,27,166*).

3.2.b. CDOM Radicals

Figure 4 shows various types of CDOM radicals being produced during irradiation. The main routes for their formation are presumed to be homolytic bond cleavage (reaction 5), formation of diradical charge-separated species (reactions 7 and 10), and oxidation by O_2

(reaction 11). Evidence for CDOM radicals comes from electron spin resonance measurements and the use of nitroxides and nitric oxide as C-centered-specific and non-specific radical probes, respectively (*53,54,142,167,168,170-173*). There have also been transient spectroscopic studies of CDOM radicals produced by reaction of •OH and e^-(aq) generated from pulse radiolysis of water (*174,175*). Some CDOM radicals are stable in the dark and are presumably semiquinones (*53,54,169*), but others are transient and have estimated lifetimes of approximately a few to several hundred μs (*142,174,175*).

There have been limited studies of CDOM radicals, so it is difficult to assess specific formation mechanisms or their overall environmental significance. Evidence suggests that alkyl radicals are not responsible for much chemistry; acetyl and methyl radical quantum yields at 350 nm are extremely low (10^{-6} to 10^{-5}) (*176*). This is also true of organic peroxides (*155*) and alkyl nitrates, which presumably derive from organic peroxyl radicals (*177-179*). Furthermore, commonly employed nitroxide probes for CDOM radicals do not turn up large amounts of C-centered radicals but rather react predominantly by one electron reduction to form the hydroxylamine (*171,176*); this reaction is analogous to the reduction of O_2 to O_2^- and occurs with at minimum twice the quantum yield of H_2O_2 (*176*), which suggests that the same reducing intermediate is responsible for both reactions (work in progress). Besides production of H_2O_2, CDOM radicals may play a role in the fate of organic contaminants. For example, CDOM peroxyl or phenoxyl radicals are potentially long-lived photooxidants whose existence is inferred from accelerated sensitized photolysis observed when probe compound concentrations decrease below approximately 1 μM (*36,180,181*). This effect is more pronounced with humic acids than with fulvic acids (*180*), the former being more aromatic and having higher molecular weights,

which suggests that terrestrial CDOM may form radicals more efficiently or of longer lifetimes than microbial CDOM.

3.2.c. Singlet Oxygen

The term singlet oxygen refers to the two lowest electronically excited states of O_2, $^1\Delta_g$ and $^1\Sigma_g^+$. Only $^1\Delta_g$ is relevant for aquatic chemistry because $^1\Sigma_g^+$ forms with low efficiency and rapidly decays to the $^1\Delta_g$ state (*182*). Production of $^1O_2$ by CDOM occurs via energy transfer from ^{3}CDOM* to ground-state O_2 (Fig. 4, reaction 8). Thus, $^1O_2$ is essentially a probe for ^{3}CDOM* states capable of undergoing this reaction; given the low energy of $^1O_2$ (94 kJ mol^{-1}), and the generally high efficiency of energy transfer from aromatic triplets to O_2 (*182,183*), it is likely that at least 30 to 50% of the ^{3}CDOM* pool leads to $^1O_2$. Besides diffusional reaction between O_2 and triplets, $^1O_2$ can also be formed via direct excitation of ground state sensitizer-O_2 complexes (*182*), but the relevance of this mechanism for CDOM photochemistry has not been demonstrated.

Because $^1O_2$ is a selective oxidant, its impact on contaminant fate is limited to particular compound classes with which it reacts rapidly (e.g., phenolates, furans, indoles, imidazoles) and to situations where it is produced in fairly high yield. However, inside the CDOM microenvironment, $^1O_2$ concentrations are orders of magnitude higher than in bulk solution (*184*), which suggests that CDOM-associated contaminants will be more susceptible to reaction with it. Furthermore, wastewater effluent CDOM tends to have a fairly high Φ_{1O2} relative to terrestrial CDOM (*130,185*), presumably due to the microbial origin of CDOM from activated sludge. This raises the possibility that rates of $^1O_2$ reactions could be enhanced in wastewater impacted streams and rivers.

Based on the structural composition of CDOM and considerations detailed in section 3.2.d, likely $^1O_2$ sensitizers are aromatic ketones and quinones, which in free solution produce $^1O_2$ quite efficiently (*183*); it should also be noted that in samples where fluorescence indicates substantial tyrosine, tryptophan or phenylalanine, these amino acids could be a significant source of $^1O_2$ (*186*). In CDOM, the $^1O_2$ quantum yield (Φ_{1O2}) lies in the approximate range of 0.01 to 0.1 depending on CDOM source, excitation wavelength (Fig. 3), and solution pH (*38,39,108,113,130,187-189*). Such low efficiencies relative to freely dissolved aromatic ketones and quinones (*183*) indicate either inefficient energy transfer from ^{3}CDOM* to O_2 or, more likely, low ^{3}CDOM* quantum yields (Φ_T). The ability of CDOM to form charge-separated species provides a mechanism to explain this, as both direct excitation of CT complexes and rapid deactivation of ^{1}CDOM* or ^{3}CDOM* to $CDOM^{+\cdot/-\cdot}$ (Fig. 4, reactions 7 and 10) would lower Φ_T and Φ_{1O2} relative to electronically independent sensitizers. In this regard, the increase in Φ_{1O2} that occurs with decreasing excitation wavelength in the visible and near-UV (*38,108,113,136*) (Fig. 3) likely reflects an increase in Φ_T with decreasing CT character of the absorption. Below 300 nm, however, Φ_T does not increase much (*189*), possibly because ^{1}CDOM* decays more rapidly by energy transfer than intersystem crossing at these wavelengths.

The efficiency of $^1O_2$ production also depends on environmental variables such as the CDOM source and pH. Typically, Φ_{1O2} is higher for microbial than terrestrial CDOM (*38,130,185*). A related trend is the molecular weight dependence of Φ_{1O2}, because microbial CDOM has lower molecular weight. The CT model explains these phenomena on the basis that increased CT absorbance and relaxation in larger CDOM molecules decreases the efficiency of ^{3}CDOM* formation and thus Φ_{1O2}. The model explains the decrease in Φ_{1O2} with increasing pH (*39,135,187*) as reflecting a lower Φ_T due to the increased likelihood of CT complex formation

447 by dissociated aromatic acids compared to the undissociated acids; it is also noteworthy that
448 dissociation decreases Φ_T and Φ_{1O2} for individual aromatic carboxylic acids, which has been
449 ascribed to intramolecular CT effects (*190,191*).

450 3.2.d. *Triplet CDOM*

451 The existence of ^{3}CDOM* states is evidenced by the production of $^1O_2$ and other
452 photoreactions typical of organic triplets, such as energy transfer to photoisomerize dienes
453 (*136,192*). The latter reaction requires triplet energies higher than approximately 200 kJ mol^{-1}.
454 Estimates of the average ^{3}CDOM* energy range from 180 to 250 kJ mol^{-1} (*136,193*). However,
455 the lower value derives from photo-acoustic spectroscopy (PAS) measurements, which detect
456 any species capable of generating heat during thermal decay to the ground state. Given the
457 opportunities for ^{1}CDOM* to relax via CT pathways and the variety of radicals produced by
458 CDOM photolysis, much of the PAS signal observed in that study (*193*) likely did not arise from
459 ^{3}CDOM*. Furthermore, room- and low-temperature phosphorescence spectra of CDOM show
460 an emission maximum near 490 nm (244 kJ mol^{-1}) (*194,195*) supporting the higher estimate of
461 the average ^{3}CDOM* energy. This energy is sufficient not only to produce $^1O_2$ and excite dienes
462 to their triplet states but also to oxidize a wide variety of compounds. Indeed, the one-electron
463 reduction potential of ^{3}CDOM* has been estimated to be approximately 1.7 V (*196*), and many
464 environmentally relevant compounds whose photolysis is sensitized by CDOM show indications
465 of ^{3}CDOM* intermediacy (*22,25,26,197-201*). In such cases, it is worth noting that complex,
466 CDOM concentration dependent oxidation kinetics can be observed because ground-state
467 CDOM sometimes inhibits contaminant oxidation, presumably by reducing the initial radical
468 produced by one electron oxidation of the contaminant by ^{3}CDOM* (*202-204*).

Natural lifetimes of ^{3}CDOM* have been estimated using both steady-state probe techniques and time-resolved spectroscopy, and reported values lie in the range of 1 to 100 μs (*37,109,140,205-207*). Regarding the time-resolved techniques, it is worth noting that despite O_2 quenching behavior suggestive of triplets, no transient signal has yet been sufficiently characterized to unequivocally identify it as ^{3}CDOM* (*139,140,205-207*). In fact, in one study a transient that was referred to as a triplet was not quenched by alkyl phenols (*206*), common probes for ^{3}CDOM*, which suggests that the signal was actually due to some other transient intermediate.

It has not yet been possible to determine absolute ^{3}CDOM* quantum yields, Φ_T. Nonetheless, using steady-state techniques and reasonable kinetic assumptions, Φ_T is estimated to lie between 0.01 and 0.1 (*108,109,192*). This is basically identical to Φ_{1O2} and seems to indicate that the ^{3}CDOM* pool generating $^1O_2$ is the same ^{3}CDOM* that directly oxidizes contaminants (Fig. 4, reaction 9). This is consistent with the fact that 2,4,6-trimethylphenol, which reacts rapidly with ^{3}CDOM*, inhibits the CDOM sensitized oxidation of fufuryl alcohol, a selective probe for CDOM-sensitized $^1O_2$ (*208*). Furthermore, the efficiency of oxidations initiated by ^{3}CDOM* also follow similar patterns with regard to CDOM source and molecular weight (*209,210*) to those described above for Φ_{1O2}. In contrast, the efficiency of phenol oxidation by ^{3}CDOM* has a pH dependence opposite to that for Φ_{1O2} (*36*). Although this could simply reflect the increasing ease of phenol oxidation as pH increases (*134*), this effect has never been experimentally distinguished from an effect of pH on Φ_T.

Most evidence suggests that aromatic ketone and quinone chromophores comprise the oxidizing ^{3}CDOM*. The case for aromatic ketones rests in large part on research by Canonica and co-workers. Oxidations of substituted phenols by well-characterized aromatic ketones and

CDOM both appear to occur by an electron transfer mechanism (*22,145,211*). Furthermore, the rate constants for these reactions follow a similar trend with phenol oxidation potential for both ^{3}CDOM* and ketone sensitizers (*145*). Strong evidence for ketone senstizers is also provided by the fact that borohydride reduced-CDOM samples display significantly reduced rates of 2,4,6-trimethylphenol oxidation (*109*). However, reduction does not completely eliminate triplet-induced oxidations or $^1O_2$ production (*108,109*). This could be attributable to quinones, which are reversibly reduced by borohydride (*97,109*); alternatively, it could result from incomplete reduction of ketone sensitizers. Evidence for quinones in CDOM comes from varied sources, including electron spin resonance (*53,54,169*) and electrochemical experiments (*59*). Whether ^{3}CDOM* is ketone- or quinone-like, the mechanism for its action as an oxidant is likely e^- transfer (Fig. 4, reaction 9). Intramolecular reactions of this type (e.g., between aromatic ketones and lignin phenols) are a potential source of $CDOM^{+\cdot/-\cdot}$ (Fig. 4, reaction 10). Whether such charge-separated species can be reached via ^{3}CDOM* is unknown. A recent report that decay rates of ^{3}CDOM* decrease with ionic strength suggests that there are Debye-Hückel type electrostatic influences on ^{3}CDOM* deactivation, which could possibly be associated with CT deactivation pathways (*212*).

3.2.e. Superoxide and Hydrogen Peroxide

The photochemical production of O_2^- and H_2O_2 by CDOM influences trace-metal redox chemistry (*213-216*) and leads to CDOM oxidation. Irradiation of various waters with natural sunlight or with comparable artificial sources (~1 to 3x solar intensities) produces both O_2^- and H_2O_2 at similar rates, which depend strongly on the water source and vary widely, from 0.5 to 10^3 nM h^{-1} (*155,217-219*); in some cases, particularly oceanic waters, biological sources of O_2^- may be significant (*220,221*). Reactions with dissolved metals and CDOM hold O_2^- at steady-

state concentrations of approximately 0.1 to 10 nM (*217,221-224*). Roughly half the O_2^- dismutates to H_2O_2 (*217,225*), a relatively stable species with diurnal maxima of high nM to μM concentrations (*138,226*). Because of this, H_2O_2 is a convenient proxy for CDOM e^- loss. Indeed, the good agreement between estimated extents of CDOM oxidation from H_2O_2 yields and DIC yields noted in section 3.1 supports this proposition.

Quantum yields for H_2O_2 (Φ_{H2O2}) have a wavelength dependence closely resembling that of the other PPRIs (Fig. 3). At approximately 350 nm, Φ_{H2O2} ranges from $0.5x10^{-4}$ to 10^{-3} for various CDOM samples (*32,39,79,138,155,219*). Quantum yields for O_2^- have not been directly established, but given the stoichiometry of dismutation and an additional 50% loss of O_2^- to other processes, a reasonable estimate of Φ_{O2-} is approximately $4\Phi_{H2O2}$. Although Φ_{H2O2} has been determined for many different waters, no systematic study exists of its CDOM source dependence. There is a reported correlation between H_2O_2 production rates and fluorescence quantum yields from lake CDOM (*219*), which suggests that lower molecular weight, less aromatic CDOM produces H_2O_2 more efficiently. However, this trend is not apparent in the limited data that exist for Φ_{H2O2} of FA (less aromatic) and HA (more aromatic) from the same source (*39,110*), nor is it the expected pattern based on the reported inverse relationship between Φ_{H2O2} and E2/E3 (*39*).

The H_2O_2 formation mechanism clearly involves the direct production of O_2^- by reaction of O_2 with some photoproduced reductant. At wavelengths above 300 nm, the involvement of e^-(aq) can be ruled out on grounds that Φ_{e-} is much smaller than Φ_{H2O2} and that e^-(aq) scavengers do not affect Φ_{H2O2} (*161,227*). Furthermore, reactions between $^1O_2$ and CDOM have repeatedly been shown to have minimal impact on H_2O_2 production (*39,110,157,225*). Other evidence argues against a role for CDOM triplet quinones as intermediates in O_2 reduction. Recently,

538 Garg *et al.* (*225*) reported that DMSO has no effect on H_2O_2 production by Suwannee River FA
539 (SRFA), yet the same group demonstrated that DMSO enhances H_2O_2 production by
540 anthraquinone disulfonate (*228*). Additionally, Zhang *et al.* reported that halides enhance H_2O_2
541 production by SRFA, which is opposite the result expected if triplet quinones were involved
542 (*110*). Zhang *et al.* also saw minimal effects of borohydride reduction and triplet quenchers on
543 H_2O_2 production rates, which demonstrates that aromatic ketones do not play an intermediate
544 role (*110*). Rather, these authors propose that the reductant is a $CDOM^{+\bullet/-\bullet}$ species formed
545 directly by intramolecular electron transfer reactions of excited singlet states (Fig. 4, reaction 7).
546 Debye-Hückel theory suggests that such a charge separated species should be stabilized at high
547 ionic strength (*229*) and have a longer lifetime, which may explain observations that increasing
548 salinity elevates both H_2O_2 production and photobleaching rates (*79,230*).

549 *3.2.f. Hydroxyl Radical*

550 Irradiated CDOM oxidizes many compounds via •OH-like reactivity (*181,231,232*). Not
551 all of this appears to be free •OH (*233,234*), so published environmental production rates, 10^{-11}
552 to 10^{-9} M s^{-1} (*235-237*) may represent a mix of free •OH and hydroxylating CDOM species; also,
553 few studies have specifically isolated the influence of CDOM from that of nitrate and nitrite.
554 There is good evidence that CDOM does produce free •OH, some of which forms through
555 Fenton-like chemistry involving H_2O_2 and a CDOM photo-reductant (*233,234*). This reductant
556 can include photochemically reduced Fe(II), particularly in acidic water, as well as reductants in
557 CDOM of unknown identity (*20,203,233,234,237,238*); semiquinones are unlikely candidates
558 because they are not known to reduce H_2O_2 to •OH (*239*). Besides Fenton chemistry, some
559 CDOM species is responsible for direct production of at least 50% of the free •OH (*233*). Again,
560 the identity of this species is unknown, but evidence argues against direct reactions of triplet

quinones, which do not photochemically produce free •OH (*240-242*). In addition to free •OH, hydroxylations also appear to occur via some lower energy CDOM species, possibly water-quinone exciplexes (*228,240,242,243*). Figure 4 thus shows various routes to •OH involving CDOM radicals; these are complex reactions, possibly involving organic peroxides, and include a role for water because hydroxylation and •OH formation cannot be eliminated under anoxic conditions (*144,181*).

The apparent quantum yield of •OH (Φ_{OH}) from CDOM (including Fenton-like chemistry) is approximately 10^{-5} to 10^{-4} in the 300 to 400 nm region (*144,237*). Its CDOM source dependence is not well explored and is difficult to assess. Many studies simply report •OH production rates upon polychromatic irradiation of waters with different CDOM levels and solution conditions. In the few cases where Φ_{OH} is reported (*88,144,244*) there are differences in pH and irradiation conditions. With polychromatic irradiation, Rosario-Ortiz and co-workers have reported that Φ_{OH} is higher for wastewater effluent OM than HS isolates (*244*) and in low molecular weight, more fluorescent fractions of wastewater OM (*88*). This suggests that •OH is produced more efficiently in samples with fewer CT interactions. Despite the similarity of this reactivity pattern to that for ^{3}CDOM*, there is no evidence that ^{3}CDOM* is involved in •OH production. In fact, the wavelength dependence of Φ_{OH} differs distinctly from that of the other PPRIs, reaching a maximum near 310 nm (*144,236,237*). More work is needed to characterize the relationship between CDOM character and Φ_{OH} and the mechanisms for •OH formation.

3.3 Relationships between CDOM Optical and Photochemical Properties

Several correlations have been reported between the quantum yields of CDOM photochemical reactions and absorption coefficients (*12,185*), specific absorption coefficients (*10,245*), spectral slope or E2/E3 (*15,39,130,246*), and fluorescence quantum yields (*88*). Such

584 correlations have potential use for predicting the photochemical reactivity of natural waters, but
585 the robustness of this approach depends on proper understanding of the underlying physical
586 basis. In this regard, the CT model may offer some insight. For example, the direct correlations
587 between Φ_{1O2} and E2/E3, spectral slope, and absorption coefficients noted by several researchers
588 (*39,130,185,246*) can be explained as reduced efficiency of ^{3}CDOM* formation in samples with
589 more CT absorbance (Fig. 4, reaction 2) and CT deactivation of ^{1}CDOM* (Fig. 4, reaction 7).
590 The inverse correlation of Φ_{H2O2} with E2/E3 (*39*) and correlations of CO quantum yields with
591 absorption and specific absorption coefficients (*10,12,245*) could potentially be the result of
592 enhanced rates of $CDOM^{+\cdot/-\cdot}$ formation (Fig. 4, reaction 7) in samples with higher levels of
593 aromatic electron donors. Alternatively, the correlation between CO production rates and
594 specific absorption may simply reflect the contribution of aromatic groups to both absorption and
595 CO production (*11,247*).

596 The correlations can also be a guide for assessing the validity of proposed pathways for
597 PPRI formation. For instance, Φ_{OH} correlates with fluorescence quantum yields (*88*). Given that
598 fluorescence yields tend to increase with E2/E3 and that E2/E3 correlates negatively with Φ_{H2O2},
599 the relationship between Φ_{OH} and fluorescence suggests that different excited states produce
600 H_2O_2 and •OH. This would seem to rule out reaction 13 in Figure 4 as a route to •OH. Also, the
601 observation that formaldehyde, acetaldehyde, acetone quantum yields correlate with spectral
602 slopes (*15*) appears to be evidence that pathways to CDOM radical precursors to these molecules
603 (Fig. 4, reaction 5) form in competition with CT deactivation of ^{1}CDOM*. Future investigations
604 of spectral-photochemical relationships using varied CDOM samples and solution conditions
605 (e.g., pH, ionic strength) should provide additional useful tests of the CT model and help
606 elucidate mechanistic aspects of CDOM photochemistry.

607 **References**

1. Aiken, G. R.; McKnight, D. M.; Wershaw, R. L.; MacCarthy, P. *Humic Subtances in Soil, Sediment, and Water;* John Wiley and Sons, 1985.

2. Blough, N. V.; Del Vecchio, R. Chromophoric DOM in the coastal environment. In *Biogeochemistry of Marine Dissolved Organic Matter;* Hansell, D. A., Carlson, C. A., Eds.; Academic Press, 2002.

3. Bidigare, R. R.; Ondrusek, M. E.; Brooks, J. M. Influence of the Orinoco River outflow on distributions of algal pigments in the Caribbean Sea. *J. Geophys. Res.: Oceans* **1993,** *98,* C2:2259-2269, DOI: 10.1029/92JC02762.

4. Arrigo, K. R.; Brown, C. W. Impact of chromophoric dissolved organic matter on UV inhibition of primary productivity in the sea. *Mar. Ecol. Prog. Ser.* **1996,** *140,* 207-216.

5. Sulzberger, B. Photooxidation of dissolved organic matter: Role for carbon bioavailability and for the penetration depth of solar UV-radiation. In *Chemical Processes in Marine Environments;* Gianguzza, A., Pelizzetti, E., Sammartano, S., Eds.; Springer, 2000.

6. Mopper, K.; Kieber, D. J. Photochemistry and cycling of carbon, sulfur, nitrogen and phosphorus. In *Biogeochemistry of Marine Dissolved Organic Matter;* Hansell, D. A., Carlson, C. A., Eds.; Academic Press, 2002.

7. Zepp, R. G.; Erickson III, D. J.; Paul, N. D.; Sulzberger, B. Interactive effects of solar UV radiation and climate change on biogeochemical cycling. *Photochem. Photobiol. Sci.* **2007,** *6,* 286-300.

8. Wang, W.; Johnson, C. G.; Takeda, K.; Zafiriou, O. C. Measuring the photochemical production of carbon dioxide from marine dissolved organic matter by pool isotope exchange. *Environ. Sci. Technol.* **2009,** *43,* 8604–8609.

9. Osburn, C. L.; Wigdahl, C. R.; Fritz, S. C.; Saros, J. E. Dissolved organic matter composition and photoreactivity in prairie lakes of the U.S. Great Plains. *Limnol. Oceanogr.* **2011,** *56,* 2371-2390.

10. Zhang, Y.; Xie, H.; Chen, G. Factors affecting the efficiency of carbon monoxide photoproduction in the St. Lawrence estuarine system (Canada). *Environ. Sci. Technol.* **2006,** *40,* 7771-7777.

11. Stubbins, A.; Hubbard, V.; Uher, G.; Law, C. S.; Upstill-Goddard, R. C.; Aiken, G. R.; Mopper, K. Relating carbon monoxide photoproduction to dissolved organic matter

functionality. *Environ. Sci. Technol.* **2008,** *42,* 3271-3276.

12. Stubbins, A.; Law, C. S.; Uher, G.; Upstill-Goddard, R. C. Carbon monoxide apparent quantum yields and photoproduction in the Tyne estuary. *Biogeosci.* **2011,** *8,* 703–713.

13. White, E. M.; Kieber, D. J.; Sherrard, J.; Miller, W. L.; Mopper, K. Carbon dioxide and carbon monoxide photoproduction quantum yields in the Delaware Estuary. *Mar. Chem.* **2010,** *118,* 11-21.

14. Ziolkowski, L. A.; Miller, W. L. Variability of apparent quantum efficiency of CO photoproduction in the Gulf of Maine and Northwest Atlantic. *Mar. Chem.* **2007,** *105,* 258-270.

15. de Bruyn, W. J.; Clark, C. D.; Pagel, L.; Takehara, C. Photochemical production of formaldehyde, acetaldehyde and acetone from chromophoric dissolved organic matter in coastal waters. *J. Photochem. Photobiol. A: Chem.* **2001,** *226,* 16-22.

16. Pullin, M. J.; Bertilsson, S.; Goldstone, J. V.; Voelker, B. M. Effects of sunlight and hydroxyl radical on dissolved organic matter: bacterial growth efficiency and production of carboxylic acids and other substrates. *Limnol. Oceanogr.* **2004,** *49,* 2011-2022.

17. Lou, T.; Xie, H. Photochemical alteration of the molecular weight of dissolved organic matter. *Chemosphere* **2006,** *65,* 2333-2342.

18. Miller, W. L.; Moran, S. A.; Sheldon, W. M.; Zepp, R. G.; Opsahl, S. Determination of the apparent quantum yields for the formation of biologically-labile photoproducts. *Limnol. Oceanogr.* **2002,** *47,* 343-352.

19. Sulzberger, B. Effects of light on the biological availability of trace metals. In *Marine Chemistry;* Gianguzza, A., Pelizzetti, E., Sammartano, S., Eds.; Kluwer Academic Publishers, 1997.

20. Voelker, B. M.; Morel, F. M. M.; Sulzberger, B. Iron redox cycling in surface waters: Effects of humic substances and light. *Environ. Sci. Technol.* **1997,** *31,* 1004-1011.

21. Gabarell, M.; Chin, Y.-P.; Hug, S. J.; Sulzberger, B. Role of dissolved organic matter composition on the photoreduction of Cr(VI) to Cr(III) in the presence of iron. *Environ. Sci. Technol.* **2003,** *37,* 4403-4409.

22. Gerecke, A. C.; Canonica, S.; Müller; Sharer, M.; Schwarzenbach, R. P. Quantification of dissolved natural organic matter (DOM) mediated phototransformation of phenylurea herbicides in lakes. *Environ. Sci. Technol.* **2001,** *35,* 3915-3923.

23. Burns, S. E.; Hassett, J. P.; Rossi, M. V. Binding effects on humic-mediated photoreaction: intrahumic dechlorination of mirex in water. *Environ. Sci. Technol.* **1996,** *30,* 2934-2941.

24. Latch, D. E.; Stender, B. L.; Arnold, W. A.; McNeill, K. Photochemical fate of pharmaceuticals in the environment: cimetidine and ranitidine. *Environ. Sci. Technol.* **2003,** *37,* 3342-3350.

25. Chin, Y.-P.; Miller, P. L.; Zeng, L.; Cawley, K.; Weavers, L. K. Photosensitized degradation of bisphenol A by dissolved organic matter. *Environ. Sci. Technol.* **2004,** *38,* 5888-5894.

26. Guerard, J. J.; Miller, P. L.; Trouts, T. D.; Chin, Y.-P. The role of fulvic acid composition in the photosensitized degradation of aquatic contaminants. *Aquat. Sci.* **2009,** *71,* 160-169.

27. Grannas, A. M.; Cory, R. M.; Miller, P. L.; Chin, Y.-P.; McKnight, D. M. The role of dissolved organic matter in arctic surface waters in the photolysis of hexachlorobenzene and lindane. *J. Geophys. Res.* **2012,** *117,* G01003, doi:10.1029/2010JG001518.

28. Packer, J. L.; Werner, J. J.; Latch, D. E.; Mcneill, K.; Arnold, W. A. Photochemical fate of pharmaceuticals in the environment: Naproxen, diclofenac, clofibric acid and ibuprofen. *Aquat. Sci.* **2003,** *65,* 342-351.

29. Boreen, A. L.; Arnold, W. A.; Mcneill, K. Photodegradation of pharmaceuticals in the environment: A review. *Aquat. Sci.* **2003,** *65,* 320-341.

30. Laane, R. W. P. M.; Gieskes, W. W. C.; Kraay, G. W.; Eversdijk, A. Oxygen consumption from natural waters by photo-oxidizing processes. *Neth. J. Sea Res.* **1985,** *19,* 125-128.

31. Obernosterer, I. R. P.; Herndl, G. J. Spatial and diurnal dynamics of dissolved organic matter (DOM) fluorescence and H_2O_2 and the photochemical oxygen demand of surface water DOM across the subtropical Atlantic Ocean. *Limnol. Oceanogr.* **2001,** *46,* 632-643.

32. Andrews, S. S.; Caron, S.; Zafiriou, O. C. Photochemical oxygen consumption in marine waters: A major sink for colored dissolved organic matter? *Limnol. Oceanogr.* **2000,** *45,* 267-277.

33. Amon, R. M. W.; Benner, R. Photochemical and microbial consumption of dissolved organic carbon in the Amazon River system. *Geochim. Cosmochim. Acta* **1996,** *60,* 1783-1792.

34. Fellman, J. B.; Hood, E.; Spencer, R. G. M. Fluorescence spectroscopy opens new windows into dissolved organic matter dynamics in freshwater ecosystems: A review. *Limnol.*

Oceanogr. **2010,** *55,* 2452-2462.

35. Nelson, N. B.; Siegel, D. A. The global distribution and dynamics of chromophoric dissolved organic matter. *Annu. Rev. Mar. Sci.* **2013,** *5,* 447-476.

36. Canonica, S.; Freiburghaus, M. Electron-rich phenols for probing the photochemical reactivity of freshwaters. *Environ. Sci. Technol.* **2001,** *35,* 690-695.

37. Wang, W.; Zafiriou, O. C.; Chan, I.-Y.; Zepp, R. G.; Blough, N. V. Production of hydrated electrons from photoionization of dissolved organic matter in natural waters. *Environ. Sci. Technol.* **2007,** *41,* 1601-1607.

38. Paul, A.; Hackbarth, S.; Vogt, R. D.; Röder, B.; Burnison, B. K.; Steinburg, C. E. W. Photogeneration of singlet oxygen by humic substances: comparison of humic substances of aquatic and terrestrial origin. *Photochem. Photobiol. Sci.* **2004,** *3,* 273-280.

39. Dalrymple, R. M.; Carfagno, A. K.; Sharpless, C. M. Correlations between dissolved organic matter optical properties and quantum yields of singlet oxygen and hydrogen peroxide. *Environ. Sci. Technol.* **2010,** *44,* 5824-5829.

40. Johannessen, S. C.; Miller, W. L. Quantum yield for the photochemical production of dissolved inorganic carbon in seawater. *Mar. Chem.* **2001,** *76,* 271-283.

41. Meunier, L.; Laubscher, H.-U.; Sulzberger, B. Effects of size and origin of natural organic matter compounds on the redox cycling of iron in sunlit waters. *Aquat. Sci.* **2005,** *67,* 292-307.

42. Thurman, E. M. *Organic Geochemistry of Natural Waters;* Martinus Nijhoff/Junk: Netherlands, 1985.

43. Schulten, H.-R.; Gleixner, G. Analytical pyrolysis of humic subtances and dissolved organic matter in aquatic systems: structure and origin. *Wat. Res.* **1999,** *33,* 2489-2498.

44. de Haan, H. Use of ultraviolet spectroscopy, gel filtration, pyrolysis/mass spectrometry and numbers of benzoate-metabolizing bacteria in the study of humification and degradation of aquatic organic matter. In *Aquatic and Terrestrial Humic Material;* Christman, R. F., Gjessing, E. T., Eds.; Ann Arbor Science, 1983.

45. MacCarthy, P.; Deluca, S. J.; Voorhees, K. J.; Malcom, R. L.; Thurman, E. M. Pyrolysis-mass spectrometry/pattern recognition on a well-characterized suite of humic substances. *Geochim. Cosmochim. Acta* **1985,** *49,* 2091-2096.

46. Mopper, K.; Stubbins, A.; Ritchie, J. D.; Bialk, H. M.; Hatcher, P. G. Advanced instrumental approaches for characterization of marine dissolved organic matter: extraction techniques, mass spectrometry, and nuclear magnetic resonance spectroscopy. *Chem. Rev.* **2007,** *107,* 419-442.

47. Remucal, C. K.; Cory, R. M.; Sander, M.; McNeill, K. Low molecular weight components in an aquatic humic substance as characterized by membrane dialysis and orbitrap mass spectrometry. *Environ. Sci. Technol.* **2012,** *46,* 9350-9359.

48. Hertkorn, N.; Benner, R.; Frommberger, M.; Schmitt-Kopplin, P.; Witt, M.; Kaiser, K.; Kettrup, A.; Hedges, J. I. Characterization of a major refractory component of marine dissolved organic matter. *Geochim. Cosmochim. Acta* **2006,** *70,* 2990-3010.

49. Stenson, A. C.; Marshall, A. G.; Cooper, W. T. Exact masses and chemical formulas of individual Suwannee River fulvic acids from ultrahigh resolution electrospray ionization Fourier transform ion cyclotron resonance mass spectrometry. *Anal. Chem.* **2003,** *75,* 1275-1284.

50. Kujawinski, E. B.; Del Vecchio, R.; Blough, N. V.; Klein, G. C.; Marshall, A. G. Probing molecular-level transformations of dissolved organic matter: insights on photochemical degradation and protozoan modification of DOM from electrospray ionization Fourier transform ion cyclotron resonance mass spectrometry. *Mar. Chem.* **2004,** *92,* 23-37.

51. Thorn, K. A.; Folan, D. W.; MacCarthy, P. *Characterization of the International Humic Substances Society standard and reference fulvic and humic acids by solution state carbon-13 (^{13}C) and hydrogen-1 (^{1}H) nuclear magnetic resonance spectrometry;* Water-Resources Investigations Report 89-4196; U.S. Geological Survey: Denver, 1989.

52. McKnight, D. M.; Andrews, E. D.; Spaulding, S. A.; Aiken, G. R. Aquatic fulvic acids in alagal-rich artic ponds. *Limnol. Oceanogr.* **1994,** *39,* 1972-1979.

53. Lakatos, B.; Tibai, T.; Meisel, J. EPR spectra of humic acids and their metal complexes. *Geoderma* **1977,** *19,* 319-338.

54. Paul, A.; Stösser, R.; Zehl, A.; Zwirnmann, E.; Vogt, R. D.; Steinberg, C. E. W. Nature and abundance of organic radicals in natural organic matter: effect of pH and irradiation. *Environ. Sci. Technol.* **2006,** *40,* 5897-5903.

55. Ritchie, J. D.; Perdue, E. M. Proton-binding study of standard and reference fulvic acids, humic acids, and natural organic matter. *Geochim. Cosmochim. Acta* **2003,** *67,* 85-96.

56. Janot, N.; Reiller, P. E.; Korshin, G. V.; Benedetti, M. F. Using spectrophotometric titrations to characterize humic acid reactivity at environmental concentrations. *Environ. Sci. Technol.* **2010,** *44,* 6782-6788.

57. Benedetti, M.; Ranville, J. F.; Ponthieu, M.; Pinheiro, J. P. Field-flow fractionation characterization and binding properties of particulate and colloidal organic matter from the Rio Amazon and Rio Negro. *Org. Geochem.* **2002,** *33,* 269-279.

58. Aeschbacher, M.; Sander, M.; Schwarzenbach, R. P. Novel electrochemical approach to assess the redox properties of humic substances. *Environ. Sci. Technol.* **2010,** *44,* 87-93.

59. Aeschbacher, M.; Vergari, D.; Schwarzenbach, R. P.; Sander, M. Electrochemical analysis of proton and electron transfer equilibria of the reducible moieties in humic acids. *Environ. Sci. Technol.* **2011,** *44,* 87-93.

60. Nebbioso, A.; Piccolo., A. Molecular characterization of dissolved organic matter (DOM): a critical review. *Anal. Bioanal. Chem.* **2013,** *405,* 109–124.

61. Sulzberger, B.; Durisch-Kaiser, E. Chemical characterization of dissolved organic matter (DOM): A prerequisite for understanding UV-induced changes of DOM absorption properties and bioavailability. *Aquat. Sci.* **2009,** *71,* 104-126.

62. Blough, N. V.; Green, S. A. Spectroscopic characterization and remote sensing of non-living organic matter. In *The Role of Nonliving Organic Matter in the Earth's Carbon Cycle;* Zepp, R. G., Sonntag, C., Eds.; Wiley & Sons, 1995.

63. Nelson, N. B.; Siegel, D. A. Chromophoric DOM in the open ocean. In *In Biogeochemistry of Marine Dissolved Organic Matter;* Hansell, D. A., Carlson, C. A., Eds.; Academic Press, 2002.

64. Del Castillo, C. E. Remote sensing of organic matter in coastal waters. In *Remote Sensing of Coastal Aquatic Environments;* Miller, R. L., Del Castillo, C. E., McKee, B. A., Eds.; Springer, 2005.

65. Coble, P. G. Marine optical biogeochemistry: The chemistry of ocean color. *Chem. Rev.* **2007,** *107,* 402-418.

66. Peuravuori, J.; Pihlaja, K. Molecular size distribution and spectroscopic properties of aquatic humic substances. *Anal. Chim. Acta* **1997,** *337,* 133-149.

67. Twardowski, M. S.; Boss, E.; Sullivan, J. M.; Donaghy, P. L. Modeling the spectral shape of absorption by chromophoric dissolved organic matter. *Mar. Chem.* **2004,** *89,* 69–88.

68. Helms, J. R.; Stubbins, A.; Ritchie, J. D.; Minor, E. C.; Kieber, D. J.; Mopper, K. Absorption spectral slopes and slope ratios as indicators of molecular weight, source, and photobleaching of chromophoric dissolved organic matter. *Limnol. Oceanogr.* **2008,** *53,* 955-969.

69. Galgani, L.; Tognazzi, A.; Rossi, C.; Ricci, M.; Galvez, J. A.; Dattilo, A. M.; Cozar, A. . B. L.; Loiselle, S. A. Assessing the optical changes in dissolved organic matter in humic lakes by spectral slope distributions. *J. Photochem. Photobiol. B: Biology* **2011,** *102,* 132-139.

70. Loiselle, S. A.; Bracchini, L.; Dattillo, A. M.; Ricci, M.; Tognazzi, A.; Cozar, A.; Rossi, C. Optical characterization of chromophoric dissolved organic matter using wavelength distribution of absorption spectral slopes. *Limnol. Oceanogr.* **2009,** *54,* 590-597.

71. Fichot, C. G.; Benner, R. A novel method to estimate DOC concentrations from CDOM absorption coefficients in coastal waters. *Geophys. Res, Lett.* **2011,** *38,* L03610, DOI: 10.1029/2010GL046152.

72. Fichot, C. G.; Benner, R. The spectral slope coefficient of chromophoric dissolved organic matter ($S_{275\text{-}295}$) as a tracer of terrigenous dissolved organic carbon in river-influenced ocean margins. *Limnol.Oceanogr.* **2012,** *57,* 1453-1466.

73. Yacobi, Y. Z.; Alberts, J. J.; Takacs, M.; McElvaine, M. Absorption spectroscopy of colored dissolved organic carbon in Georgia (USA) rivers: the impact of molecular size distribution. *J. Limnol.* **2003,** *62,* 41-46.

74. Boyle, E. S.; Guerriero, N.; Thiallet, A.; Del Vecchio, R.; Blough, N. V. Optical properties of humic substances and CDOM: relation to structure. *Environ. Sci. Technol.* **2009,** *43,* 2262-2268.

75. Dalzell, B. J.; Minor, E. C.; Mopper, K. M. Photodegradation of estuarine dissolved organic matter: a multi-method assessment of DOM transformation. *Org. Geochem.* **2009,** *40,* 243-257.

76. Yan, M.; Korshin, G.; Wang, D.; Cai, Z. Characterization of dissolved organic matter using high-performance liquid chromatography (HPLC)–size exclusion chromatography (SEC) with a multiple wavelength absorbance detector. *Chemosphere* **2012,** *2012,* 879-885.

77. Del Vecchio, R.; Blough, N. V. Photobleaching of chromophoric dissolved organic matter in natural waters: kinetics and modeling. *Mar. Chem.* **2002,** *78,* 231-253.

78. Tzortziou, M.; Osburn, C. L.; Neale, P. J. Photobleaching of dissolved organic material from a tidal marsh-estuarine system of the Chesapeake Bay. *Photochem. Photobiol.* **2007,**

83, 782-792.

79. Osburn, C. L.; O'Sullivan, D. W.; Boyd, T. J. Increases in the longwave photobleaching of chromophoric dissolved organic matter in coastal waters. *Limnol. Oceanogr.* **2009,** *54,* 145-159.

80. Helms, J. R.; Stubbins, A.; Perdue, E. M.; Green, N. W.; Chen, H.; Mopper, K. Photochemical bleaching of oceanic dissolved organic matter and its effect on absorption spectral slope and fluorescence. *Mar. Chem.* **2013,** *155,* 81-91.

81. Brinkmann, T.; Sartorius, D.; Frimmel, F. H. Photobleaching of humic rich dissolved organic matter. *Aquat. Sci.* **2003,** *65,* 415-424.

82. Andrew, A. A.; Del Vecchio, R.; Subramaniam, A.; Blough, N. V. Chromophoric dissolved organic matter (CDOM) in the equatorial Atlantic Ocean: Optical properties and their relation to CDOM structure and source. *Mar. Chem.* **2013,** *148,* 33-43.

83. Weishaar, J. L.; Aiken, G. R.; Bergamaschi, B. A.; Fram, M. S.; Fujii, R.; Mopper, K. Evaluation of specific ultraviolet absorption as an indicator of the chemical composition and reactivity of dissolved organic carbon. *Environ. Sci. Technol.* **2003,** *37,* 4702-4708.

84. Chin, Y.-P.; Aiken, G.; O'Loughlin, E. O. Molecular weight, polydispersity, and spectroscopic properties of aquatic humic substances. *Environ. Sci. Technol.* **1994,** *28,* 1854-1858.

85. Del Vecchio, R.; Blough, N. V. On the origin of the optical properties of humic substances. *Environ. Sci.Technol.* **2004,** *38,* 3885-3891.

86. Mobed, J. J.; Hemmingsen, S. L.; Autry, J. L.; McGown, L. B. Fluorescence characterization of IHSS humic substances: total luminescence spectra with absorbance correction. *Environ. Sci. Technol.* **1996,** *30,* 3061-3065.

87. Green, S. A.; Blough, N. V. Optical absorption and emission properties of chromophoric dissolved organic matter in natural waters. *Limnol. Oceanogr.* **1994,** *39,* 1903-1916.

88. Lee, E.; Glover, C. M.; Rosario-Ortiz, F. L. Photochemical formation of hydroxyl radical from effluent organic matter: role of composition. *Environ. Sci. Technol.* **2013,** *47*, 12073-12080.

89. Mignone, R. A.; Martin, M. V.; Moran Vieyra, F. E.; Palazzi, V. I.; Lopez de Mishima, B.; Martire, D. O.; Borsarelli, C. D. Modulation of optical properties of dissolved humic substances by their molecular complexity. *Photochem. Photobiol.* **2012,** *88,* 792-800.

90. Frimmel, F. H.; Kumke, M. U. Fluorescence decay of humic substances. A comparative study. In *Humic Substances: Structure,Properties and Uses;* Davies, G., Gabhour, E., Eds.; Royal Society of Chemistry, 1998.

91. Chen, W.; Westerhoff, P.; Leenheer, J. A.; Booksh, K. Fluorescence excitation-emission matrix integration to quantify spectra for dissolved organic matter. *Environ. Sci. Technol.* **2003,** *37,* 5701-5710.

92. Cory, R.; McKnight, D. Fluorescence spectroscopy reveals ubiquitous presence of oxidized and reduced quinones in dissolved organic matter. *Environ. Sci. Technol.* **2005,** *39,* 8142-8149.

93. Goldman, J. H.; Rounds, S. A.; Needoba, J. A. Applications of fluorescence spectroscopy for predicting percent wastewater in an urban stream. *Environ. Sci. Technol.* **2012,** *46,* 4374-4381.

94. Sharpless, C. M. *Studies on the relationship between humic acid fluorescence, their physical properties, and the effects of metal complexation.;* Ph.D. Dissertation; Duke University, 1999.

95. Kouassi, A. M.; Zika, R. G. Light-induced alteration of the photophysical properties of dissolved organic matter in seawater. Part I. Photoreversible properties of natural water fluorescence. *Neth. J. Sea Res.* **1990,** *27,* 25-32.

96. Moran, M. A.; Sheldon, W. M. J.; Zepp, R. G. Carbon loss and optical property changes during long-term photochemical and biological degradation of estuarine dissolved organic matter. *Limnol. Oceanogr.* **2000,** *45,* 1254-1264.

97. Ma, J.; Del Vecchio, R.; Golanoski, K. S.; Boyle, E. S.; Blough, N. V. Optical properties of humic substances and CDOM: effects of borohydride reduction. *Environ. Sci. Technol.* **2010,** *44,* 5395-5402.

98. Stedmon, C. A.; Bro, R. Tracing dissolved organic matter in aquatic environments using a new approach to fluorescence spectroscopy. *Mar. Chem.* **2003,** *82,* 239-254.

99. Stedmon, C. A.; Bro, R. Characterizing dissolved organic matter fluorescence with parallel factor analysis: a tutorial. *Limnol. Oceanogr. Methods* **2008,** *6,* 572-579.

100. Woods, G. C.; Simpson, M. J.; Koerner, P. J.; Napoli, A.; Simpson, A. J. HILIC-NMR: Toward the identification of individual molecular components in dissolved organic matter. *Environ. Sci. Technol.* **2011,** *45,* 3880–3886.

101. Maurer, F.; Christl, I.; Kretzschmar, R. Reduction and reoxidation of humic acid: Influence on spectroscopic properties and proton binding. *Environ. Sci. Technol.* **2010,** *44,* 5787–5792.

102. Blough, N. V.; Del Vecchio, R. Comment on "HILIC-NMR: Toward identification of individual molecular components in dissolved organic matter". *Environ. Sci. Technol.* **2011,** *45,* 5908-5909.

103. Macalady, D. L.; Walton-Day, K. Redox chemistry and natural organic matter (NOM): geochemists' dream, analytical chemists' nightmare. In *Aquatic Redox Chemistry;* Tratnyek, P. G., Grundl, T. J., Haderlein, S. B., Eds.; American Chemical Society, 2011; Vol. 1071.

104. Maie, N.; Yamashita, Y.; Cory, R. M.; Boyer, J. N.; Jaffé, R. Application of excitation emission matrix fluorescence monitoring in the assessment of spatial and seasonal drivers of dissolved organic matter composition: Sources and physical disturbance controls. *Appl. Geochem.* **2012,** *27,* 917-929.

105. Chen, M.; Price, R. M.; Yamashita, Y.; Jaffé, R. Comparative study of dissolved organic matter from groundwater and surface water in the Florida coastal Everglades using multi-dimensional fluorescence combined with multivariate statistics. *Appl. Geochem.* **2010,** *25,* 872-880.

106. Jørgensen, L.; Stedmon, C. A.; Kragh, T.; Markager, S.; Middelboe, M.; Søndergaard, M. Global trends in the fluorescence characteristics and distribution of marine dissolved organic matter. *Mar. Chem.* **2011,** *126,* 139-148.

107. Goldstone, J. V.; Del Vecchio, R.; Blough, N. V.; Voelker, B. M. A multicomponent model of chromophoric dissolved organic matter photobleaching. *Photochem. Photobiol.* **2004,** *80,* 52-60.

108. Sharpless, C. M. Lifetimes of triplet dissolved natural organic matter (DOM) and the effect of $NaBH_4$ reduction on singlet oxygen quantum yields: Implications for DOM photophysics. *Environ. Sci. Technol.* **2012,** *46,* 4466-4473.

109. Golanoski, K.; Fang, S.; Del Vecchio, R.; Blough, N. V. Investigating the mechanism of phenol photooxidation by humic substances. *Environ. Sci. Technol.* **2012,** *46,* 3912-3920.

110. Zhang, Y.; Del Vecchio, R.; Blough, N. V. Investigating the mechanism of hydrogen peroxide photoproduction by humic substances. *Environ. Sci. Technol.* **2012,** *46,* 11836-11843.

111. Thomas-Smith, T. E.; Blough, N. V. Photoproduction of hydrated electron from constituents of natural waters. *Environ. Sci. Technol.* **2001,** *35,* 2721-2726.

112. Reader, H. E.; Miller, W. L. Variability of carbon monoxide and carbon dioxide apparent quantum yield spectra in three coastal estuaries of the South Atlantic Bight. *Biogeosciences* **2012,** *9,* 4279-4294.

113. Haag, W. R.; Hoigné, J.; Gassman, E.; Braun, A. M. Singlet oxygen in surface waters – part II: quantum yields of its production by some natural humic materials as a function of wavelength. *Chemosphere* **1984,** *13,* 641-650.

114. Sleighter, R. L.; Hatcher, P. G. Molecular characterization of dissolved organic matter (DOM) along a river to ocean transect of the lower Chesapeake Bay by ultrahigh resolution electrospray ionization Fourier transform ion cyclotron resonance mass spectrometry. *Mar. Chem.* **2008,** *110,* 140−152.

115. Kujawinski, E. B.; Longnecker, K.; Blough, N. V.; Del Vecchio, R.; Finlay, L.; Kitner, J. B.; Giovannoni, S. J. Identification of possible source markers in marine dissolved organic matter using ultrahigh resolution mass spectrometry. *Geochim. Cosmochim. Acta* **2009,** *73,* 4384−4399.

116. Baluha, D. R.; Blough, N. V.; Del Vecchio, R. Selective mass labeling for linking optical properties of chromophoric dissolved organic matter to structure and composition via ultrahigh resolution electrospray mass spectrometry. *Environ. Sci. Technol.* **2013,** *47,* 9891-9897.

117. Abdulla, H. A. N.; Minor, E.; Dias, R.; Hatcher, P. G. Transformation of the chemical compositions of high molecular weight DOM along a salinity transect: using two dimensional correlation spectroscopy and principal component analysis approaches. *Geochim. Cosmochim. Acta* **2013,** *118,* 231-246.

118. Herzsprung, P.; von Tümpling, W.; Hertkorn, N.; Harir, M.; Büttner, O.; Bravidor, J.; Friese, K.; Schmitt-Kopplin, P. Variations of DOM quality in inflows of a drinking water reservoir: linking of van Krevelen diagrams with EEMF spectra by rank correlation. *Environ. Sci. Technol.* **2012,** *46,* 5511-5518.

119. Spencer, R. G. M.; Aiken, G. R.; Wickland, K. P.; Striegl, R. G.; Hernes, P. J. Seasonal and spatial variability in dissolved organic matter quantity and composition from the Yukon River basin, Alaska. *Global Biogeochem. Cycles* **2008,** *22,* GB4002, DOI:10.1029/2008gb003231.

120. Hernes, P. J.; Spencer, R. G. M.; Dyda, R. Y.; Pellerin, B. A.; Bachand, P. A. M.; Bergamaschi, B. A. The role of hydrologic regimes on dissolved organic carbon composition in an agricultural watershed. *Geochim. Cosmochim. Acta* **2008,** *72,* 5266–5277.

121. Spencer, R. G. M.; Hernes, P. J.; Ruf, R.; Baker, A.; Dyda, R. Y.; Stubbins, A.; Six, J. Temporal controls on dissolved organic matter and lignin biogeochemistry in a pristine tropical river, Democratic Republic of Congo. *J. Geophys. Res. Biogeosci.* **2010,** *115,* G03013, DOI: 10.1029/2009JG001180.

122. Spencer, R. G. M.; Stubbins, A.; Hernes, P. J.; Baker, A.; Mopper, K.; Aufdenkampe, A. K.; Dyda, R. Y.; Mwamba, V. L.; Mangangu, A. M.; Wabakanghanzi, J. N.; Six, J. Photochemical degradation of dissolved organic matter and dissolved lignin phenols from the Congo River. *J. Geophys. Res.* **2009,** *114,* G03010, doi:10.1029/2009JG000968.

123. Hernes, P. J.; Benner, R. Photochemical and microbial degradation of dissolved lignin phenols: Implications for the fate of terrigenous dissolved organic matter in marine environments. *J. Geophys. Res., Oceans* **2003,** *108,* 3291, DOI:10.1029/2002JC001421.

124. Birks, J. B. In *Photophysics of Aromatic Molecules;* Wiley-Interscience, 1970; Chapter 9.

125. Malkin, J. In *Photophysical and Photochemical Properties of Aromatic Compounds.;* CRC Press: Boca Raton, 1992; Chaps. 10 & 12.

126. Korshin, G. V.; Benjamin, M. M.; Li, C.-W. Use of differential spectroscopy to evaluate the structure and reactivity of humics. *Wat. Sci. Technol.* **1999,** *40,* 9-16.

127. Furman, G. S.; Lonsky, W. F. W. Charge-transfer complexes in kraft lignin part 2: contribution to color. *J. Wood Chem. Technol.* **1988,** *8,* 191-208.

128. Korshin, G. V.; Li, C.-W.; Benjamin, M. M. Monitoring the properties of natural organic matter through UV spectroscopy: a consistent theory. *Wat. Res.* **1997,** *31,* 1787-1795.

129. Wenk, J.; Aeschbacher, M.; Salhi, E.; Canonica, S.; von Gunten, U.; Sander, M. Chemical oxidation of dissolved organic matter by chlorine dioxide, chlorine, and ozone: effects on its optical and antioxidant properties. *Environ. Sci. Technol.* **2013,** *47,* 11147-11156.

130. Mostafa, S.; Rosario-Ortiz, F. L. Singlet oxygen formation from wastewater organic matter. *Environ. Sci. Technol.* **2013,** *47,* 8179-8186.

131. Korshin, G. V.; Kumke, M. U.; Li, C.-W.; Frimmel, F. H. Influence of chlorination on chromophores and fluorophores in humic substances. *Environ. Sci. Technol.* **1999,** *33,* 1207-1212.

132. Dryer, D. J.; Korshin, G. V.; Fabbricino, M. In situ examination of the protonation behavior of fulvic acids using differential absorbance spectroscopy. *Environ. Sci. Technol.* **2008,** *42,* 6644-6649.

133. Wehry; E.L.; Rogers; L.B. Application of linear free energy relations to electronically-excited states of mono-substituted phenols. *J. Am. Chem. Soc.* **1965,** *87,* 4234-4238.

134. Li, C.; Hoffman, M. Z. One electron oxidation potentials of phenols in aqueous solution. *J. Phys. Chem. B* **1999,** *103,* 6653-6656.

135. Zepp, R. G.; Baughman, G. L.; Schlotzhauer, P. F. Comparison of photochemical behavior of various humic substances in water: II. Photosensitized oxygenations. *Chemosphere* **1981,** *10,* 119-126.

136. Zepp, R. G.; Schlotzhauer, P. F.; Sink, R. M. Photosensitized transformations involving electronic energy transfer in natural waters: Role of humic substances. *Environ. Sci. Technol.* **1985,** *19,* 74-81.

137. Cooper, W. J.; Zika, R. G. Photochemical formation of hydrogen peroxide in surface and ground waters exposed to sunlight. *Science* **1983,** *220,* 711-712.

138. Cooper, W. J.; Zika, R. G.; Petasne, R. G.; Plane, J. M. C. Photochemical formation of H_2O_2 in natural waters exposed to sunlight. *Environ. Sci. Technol.* **1988,** *22,* 1156-1160.

139. Fischer, A.; Kliger, D.; Winterle, J.; Mill, T. Direct observations of phototransients in natural waters. *Chemosphere* **1985,** *14,* 1299-1306.

140. Power, J. F.; Sharma, D. K.; Langford, C. H.; Bonneau, R.; Joussot-Dubien, J. Laser flash photolysis studies of a well-characterized soil humic substance. In *Photochemistry of Environmental Aquatic Systems: ACS Symposium Series;* Zika, R. G., Cooper, W. J., Eds.; American Chemical Society, 1987; Vol. 327.

141. Zafirou, O. C.; Jousset-Dubien, J.; Zepp, R. G.; Zika, R. G. Photochemistry of natural waters. *Environ. Sci. Technol.* **1984,** *18,* A358-A371.

142. Blough, N. V. Electron paramagnetic resonance measurements of photochemical radical production in humic substances. 1. Effects of O_2 and charge on radical scavenging by nitroxides. *Environ. Sci. Technol.* **1988,** *22,* 77-82.

143. Mopper, K.; Zhou, X. Hydroxyl radical photoproduction in the sea and its potential impact on marine processes. *Science* **1990,** *250,* 661-664.

144. Vaughan, P. P.; Blough, N. V. Photochemical formation of hydroxyl radical by constituents of natural waters. *Environ. Sci. Technol.* **1998,** *32,* 2947-2953.

145. Canonica, S.; Jans, U.; Stemmler, K.; Hoigné, J. Transformation kinetics of phenols in water: photosensitization by dissolved natural organic material and aromatic ketones. *Environ. Sci. Technol.* **1995,** *29,* 1822-1831.

146. Zafiriou, O. C.; Blough, N. V.; Micinski, E.; Dister, B.; Kieber, D.; Moffett, J. Molecular probe systems for reactive transients in natural waters. *Mar. Chem.* **1990,** *30,* 45-70.

147. Blough, N. V.; Zepp, R. G. Reactive oxygen species in natural waters. In *In Active Oxygen in Chemistry;* Foote, C. S., Valentine, J. S., Greenberg, A., Liebman, J. F., Eds.; Chapman & Hall, 1995.

148. Burns, J. M.; Cooper, W. J.; Ferry, J. L.; King, D. W.; DiMento, B. P.; McNeill, K.; Miller, C. J.; Miller, W. L.; Peake, B. M.; Rusak, S. A.; Rose, A. L.; Waite, T. D. Methods for reactive oxygen species (ROS) detection in aqueous environments. *Aquat. Sci.* **2012,** *74,* 683-734.

149. Kouassi, A. M.; Zika, R. G.; Plane, J. M. C. Light-induced alteration of the photophysical properties of dissolved organic matter in seawater: Part II. Estimates of the environmental rates of the natural water fluorescence. *Neth. J. Sea Res.* **1990,** *27,* 33-41.

150. Opsahl, S.; Benner, R. Photochemical reactivity of dissolved lignin in river and ocean waters. *Limnol. Oceanogr.* **1998,** *43,* 1297-1304.

151. Scully, N. M.; Maie, N.; Dailey, S. K.; Boyer, J. N.; Jones, R. D.; Jaffé, R. Early diagenesis of plant-derived dissolved organic matter along a wetland, mangrove, estuary ecotone. *Limnol. Oceanogr.* **2004,** *49,* 1667–1678.

152. Stubbins, A.; Spencer, R. G. M.; Chen, H.; Hatcher, P. G.; Mopper, K.; Hernes, P. J.; Mwamba, V. L.; Mangangu, A. M.; Wabakanghanzi, J. N.; Six, J. Illuminated darkness: molecular signatures of Congo River dissolved organic matter and its photochemical alteration as revealed by ultrahigh precision mass spectrometry. *Limnol. Oceanogr.* **2010,** *55,* 1467-1477.

153. Thorn, K. A.; Younger, S. J.; Cox, L. G. Order of functionality loss during photodegradation of aquatic humic substances. *J. Environ. Qual.* **2010,** *39,* 1416-1428.

154. Osburn, C. L.; Retamal, L.; Vincent, W. F. Photoreactivity of chromophoric dissolved organic matter transported by the Mackenzie River to the Beaufort Sea. *Mar. Chem.* **2009,**

115, 10-20.

155. O'Sullivan, D. W.; Neale, P. J.; Coffin, R. B.; Boyd, T. J.; Osburn, C. L. Photochemical production of hydrogen peroxide and methylhydroperoxide in coastal waters. *Mar. Chem.* **2005,** *97,* 14-33.

156. Gao, H.; Zepp, R. G. Factors influencing photoreactions of dissolved organic matter in a coastal river of the southeastern United States. *Environ. Sci. Technol.* **1998,** *32,* 2940-2946.

157. Cory, R. M.; McNeill, K.; Cotner, J. B.; Amado, A.; Purcell, J. M.; Marshall, A. G. Singlet oxygen in the coupled photochemical and biological oxidation of dissolved natural organic matter. *Environ. Sci. Technol.* **2010,** *44,* 3683-3689.

158. Goldstone, J. V.; Pullin, M. J.; Bertilsson, S.; Voelker, B. M. Reactions of hydroxyl radical with humic substances: bleaching, mineralization, and production of bioavailable carbon substrates. *Environ. Sci. Technol.* **2002,** *36,* 364-372.

159. Hefner, K. H.; Fisher, J. M.; Ferry, J. L. A multifactor exploration of the photobleaching of Suwannee River dissolved organic matter across the freshwater/saltwater interface. *Environ. Sci. Technol.* **2006,** *40,* 3717-3722.

160. Loiselle, S.; Vione, D.; Minero, C.; Maurino, V.; Tognazzi, A.; Dattilo, A. M.; Rossi, C.; Bracchini, L. Chemical and optical phototransformation of dissolved organic matter. *Wat. Res.* **2012,** *46,* 3197-3207.

161. Zepp, R. G.; Braun, A. M.; Hoigné, J.; Leenheer, J. A. Photoproduction of hydrated electrons from natural organic solutes in aquatic environments. *Environ. Sci. Technol.* **1987,** *21,* 485-490.

162. Aguer, J. P.; Richard, C. Photochemical behaviour of a humic acid synthesized from phenol. *J. Photochem. Photobiol. A: Chem.* **1994,** *84,* 69-73.

163. Fisher, A. M.; Winterle, J. S.; Mill, T. Primary photochemical processes in photolysis mediated by humic substances. In *Photochemistry of Environmental Aquatic Systems (ACS Symposium Series);* Zika, R. G., Cooper, W. J., Eds.; American Chemical Society: Washington, DC, 1987; Vol. 327, pp 141-156.

164. Kohler, G.; Solar, S.; Getoff, N.; Holzwarth, A. R.; Schaffner, K. J. Relationship between the quantum yields of electron photoejection and fluorescence of aromatic carboxylate anions in aqueous solution. *J. Photochem.* **1985,** 383-391.

165. Mossoba, M.; Makino, K.; Riesz, P. Photoionization of aromatic amino acids in aqueous

solutions. A spin-trapping, and electron spin resonance study. *J. Phys. Chem.* **1982,** *86,* 3478–3483.

166. Burns, S. E.; Hassett, J. P.; Rossi, M. V. Mechanistic implications of the intrahumic dechlorination of Mirex. *Environ. Sci. Technol.* **1997,** *31,* 1365-1371.

167. Slawinska, D.; Slawinski, J.; Sarna, T. The effect of light on the ESR spectra of humic acids. *J. Soil Sci.* **1975,** *26,* 93-99.

168. Dister, B.; Zafiriou, O. C. Photochemical free radical production in the eastern Caribbean. *J. Geophys. Res.* **1993,** *98,* 2341-2352.

169. Scott, D. T.; McKnight, D. M.; Blunt-Harris, E. L.; Kolesar, S. E.; Lovley, D. R. Quinone moieties act as electron acceptors in the reduction of humic substances by humics-reducing microorganisms. *Environ. Sci. Technol.* **1998,** *32,* 2984-2989.

170. Kieber, D. J.; Blough, N. V. Determination of carbon-centered radicals in aqueous solution by liquid chromatography with fluorescence detection. *Anal. Chem.* **1990,** *62,* 2275-2283.

171. Johnson, C. G.; Caron, S.; Blough, N. V. Combined liquid chromatography/mass spectrometry of the radical adducts of a fluorescamine-derivatized nitroxide. *Anal. Chem.* **1996,** *68,* 867.

172. Senesi, N.; Chen, Y.; Schnitzer, M. Role of free radicals in oxidation and reduction of fulvic acid. *Soil Biol. Biochem.* **1977,** *9,* 397-403.

173. Wilson, S. A.; Weber, J. H. Electron spin resonance analysis of semiquinone free radicals of aquatic and soil fulvic and humic acids. *Anal. Lett.* **1977,** *10,* 75-84.

174. Cooper, W. J.; Song, W.; Gonsior, M.; Kalnina, D.; Peake, B. M.; Mezyk, S. P. Recent advances in structure and reactivity of dissolved organic matter in natural waters. *Water Sci. Technol.: Water Supply-WSTWS* **2008,** *8,* 615–623.

175. Ayatollahi, S.; Kalnina, D.; Song, W.; Cottrell, B. A. . G. M.; Cooper, W. J. Recent advances in structure and reactivity of dissolved organic matter: radiation chemistry of non-isolated natural organic matter and selected model compounds. *Water Sci. Technol.: Water Supply-WSTS* **2012,** *66,* 1941-1949.

176. Blough, N. V. Photochemistry in the sea surface microlayer. In *The Sea Surface and Global Change;* Liss, P. S., Duce, R. A., Eds.; Cambridge University Press, 1997.

177. Moore, R. M.; Blough, N. V. A marine source of methyl nitrate. *Geophys. Res. Lett.* **2002,**

29, 27-1, DOI: 10.1029/2002GL014989.

178. Dahl, E. E.; Saltzman, E. S.; de Bruyn, W. J. The aqueous phase yield of alkyl nitrates from ROO + NO: Implications for photochemical production from seawater. *Geophys. Res. Lett.* **2003,** *30,* 4-1, DOI 10.1029/2002GL016811.

179. Dahl, E. E.; Saltzman, E. S. Alkyl nitrate photochemical production rates in North Pacific seawater. *Mar. Chem.* **2008,** *112,* 137-141.

180. Canonica, S.; Hoigné, J. Enhanced oxidation of methoxy phenols at micromolar concentration photosensitized by dissolved natural organic matter. *Chemosphere* **1995,** *30,* 2365-2374.

181. Jacobs, L. E.; Weavers, L. K.; Houtz, E. F.; Chin, Y.-P. Photosensitized degradation of caffeine: Role of fulvic acids and nitrate. *Chemosphere* **2012,** *86,* 124-129.

182. Schweitzer, C.; Schmidt, R. Physical mechanisms of generation and deactivation of singlet oxygen. *Chem. Rev.* **2003,** *103,* 1685-1757.

183. Wilkinson, F. Quantum yields for the photosensitized formation of the lowest electronically excited singlet state of molecular oxygen in solution. *J. Phys. Chem. Ref. Data* **1993,** *22,* 113-262.

184. Grandbois, M.; Latch, D. E.; McNeill, K. Microheterogeneous concentrations of singlet oxygen in natural organic matter isolate solutions. *Environ. Sci. Technol.* **2008,** *42,* 9184-9190.

185. Haag, W. R.; Hoigné, J. Singlet oxygen in surface waters. 3. Photochemical formation and steady-state concentrations in various types of waters. *Environ. Sci. Technol.* **1986,** *20,* 341-348.

186. Chin, K. K.; Trevithick-Sutton, C. C.; McCallum, J.; Jockusch, S.; Turro, N. J.; Scaiano, J. C.; Foote, C. S.; Garcia-Garibay, M. A. Quantitative determination of singlet oxygen generated by excited state aromatic amino acids, proteins, and immunoglobulins. *J. Am. Chem. Soc.* **2008,** *130,* 6912-6913.

187. Frimmel, F. H.; Bauer, H.; Putzien, J.; Murasecco, P.; Braun, A. M. Laser flash photolysis of dissolved aquatic humic material and the sensitized production of singlet oxygen. *Environ. Sci. Technol.* **1987,** *21,* 541-545.

188. Sandvik, S. H.; Bilski, P.; Pakulski, J. D.; Chignell, C. F.; Coffin, R. B. Photogeneration of singlet oxygen and free radicals in dissolved organic matter isolated from the Mississippi

and Atchafalaya River plumes. *Mar. Chem.* **2000,** *69,* 139-152.

189. Lester, Y.; Sharpless, C. M.; Mamane, H.; Linden, K. G. Production of photo-oxidants by dissolved organic matter during UV water treatment. *Environ. Sci. Technol.* **2013,** *47*, 11726-11733.

190. Ehrenberg, B.; Anderson, J. L.; Foote, C. S. Kinetics and yield of singlet oxygen photosensitized by hypericin in organic and biological media. *Photochem. Photobiol.* **1998,** *68,* 135-140.

191. de la Peña, D.; Marti, C.; Nonell, S.; Martinez, L. A.; Miranda, M. A. Time-resolved near infrared studies on singlet oxygen production by the photosensitizing 2-arylpropionic acids. *Photochem. Photobiol.* **1997,** *65,* 828-832.

192. Grebel, J. E.; PIgnatello, J. J.; Mitch, W. A. Sorbic acid as a quantitative probe for the formation, scavenging and steady-state concentrations of the triplet excited state of organic compounds. *Wat. Res.* **2011,** *45,* 6535-6544 (and corrigendum, Wat. Res. 2012, 46, 4569).

193. Bruccoleri, A.; Pant, B. C.; Sharma, D. K.; Langford, C. H. Evaluation of primary photoproduct quantum yields in fulvic acid. *Environ. Sci. Technol.* **1993,** *27,* 889-894.

194. Mazhul, V. M.; Ivashkevich, L. S.; Shcherbin, D. G.; Pavlovskaya, N. A.; Naumova, G. V.; Ovchinnikova, T. F. Luminescence properties of humic substances. *J. Appl. Spectrosc.* **1997,** *64,* 503-508.

195. Del Vecchio, R. *Chromophoric dissolved organic matter (CDOM) in natural waters: distribution, dynamics and nature.;* Ph.D. dissertation; University of Maryland: College Park, 2002.

196. Canonica, S.; Hellrung, B.; Müller, P.; Wirz, J. Aqueous oxidation of phenylurea herbicides by triplet aromatic ketones. *Environ. Sci. Technol.* **2006,** *40,* 6636-6641.

197. Guerard, J. J.; Chin, Y.-P.; Mash, H.; Hadad, C. M. Photochemical fate of sulfadimethoxine in aquaculture waters. *Environ. Sci. Technol.* **2009,** *43,* 8587-8592.

198. Boreen, A. L.; Edhlund, B. L.; Cotner, J. B.; McNeill, K. Indirect photodegradation of dissolved free amino acids: The contribution of singlet oxygen and the differential reactivity of DOM from various sources. *Environ. Sci. Technol.* **2008,** *42,* 5492-5498.

199. Chen, Y.; Hu, C.; Hu, X.; Qu, J. Indirect photodegradation of amine drugs in aqueous solution under simulated sunlight. *Environ. Sci. Technol.* **2009,** *43,* 2760-2765.

200. Canonica, S. Oxidation of aquatic organic contaminants induced by excited triplet states. *Chimia* **2007,** *61,* 641-644.

201. Richard, C.; Canonica, S. Aquatic phototransformation of organic contaminants induced by coloured dissolved organic matter. In *Handbook of Environmental Chemistry, vol. 2, Part M;* Hutzinger, O., Ed.; Springer-Verlag: Berlin, 2005.

202. Canonica, S.; Laubscher, H.-U. Inhibitory effect of dissolved organic matter on triplet-induced oxidation of aquatic contaminants. *Photochem. Photobiol. Sci.* **2008,** *7,* 547-551.

203. Vermilyea, A. W.; Voelker, B. M. Photo-fenton reaction at near neutral pH. *Environ. Sci. Technol.* **2009,** *43,* 6927-6933.

204. Wenk, J.; von Gunten, U.; Canonica, S. Effect of dissolved organic matter on the transformation of contaminants induced by excited triplet states and the hydroxyl radical. *Environ. Sci. Technol.* **2011,** *45,* 1334-1340.

205. Chaikovskaya, O. N.; Levin, P. P.; Sul´timova, N. B.; Sokolova, I. V.; Kuz´min, A. V. Triplet states of humic acids studied by laser flash photolysis using different excitation wavelengths. *Russ. Chem. Bull.* **2004,** *53,* 313-317.

206. Sul'timova, N. B.; Levin, P. P.; Chaikovskaya, O. N.; Sokolova, I. V. Laser photolysis study of the triplet states of fulvic acids in aqueous solutions. *High Energy Chem.* **2008,** *42,* 464-468.

207. Cottrell, B. A.; Timko, S. A.; Devera, L.; Robinson, A. K.; Gonsior, M.; Vizenor, A. E.; Simpson, A. J. . C. W. J. Photochemistry of excited-state species in natural waters: A role for particulate organic matter. *Wat. Res.* **2013,** *47,* 5189-5199.

208. Halladja, S.; ter Halle, A.; Aguer, J.-P.; Boulkamh, A.; Richard, C. Inhibition of humic substances mediated photooxygenation of furfuryl alcohol by 2,4,6-trimethylphenol. Evidence for reactivity of the phenol with humic triplet excited states. *Environ. Sci. Technol.* **2007,** *41,* 6066–6073.

209. Richard, C.; Trubetskaya, O.; Trubetskoj, O.; Reznikova, O.; Afanas'eva, G.; Aguer, J. P.; Guyot, G. Key role of the low molecular size fraction of soil humic acids for fluorescence and photoinductive activity. *Environ. Sci. Technol.* **2004,** *38,* 2052-2057.

210. Aguer, J.-P.; Richard, C.; Trubetskaya, O.; Trubetskoj, O.; Lévèque, J.; Andreux, F. Photoinductive efficiency of soil extracted humic and fulvic acids. *Chemosphere* **2002,** *49,* 259-262.

211. Canonica, S.; Hellrung, B.; Wirz, J. Oxidation of phenols by triplet aromatic ketones in aqueous solution. *J. Phys. Chem. A* **2000,** *104,* 1226-1232.

212. Parker, K. M.; Pignatello, J. J.; Mitch, W. A. Influence of ionic strength on triplet-state natural organic matter loss by energy transfer and electron transfer pathways. *Environ. Sci. Technol.* **2013,** *47*, 10987-10994.

213. Rose, A. L.; Waite, T. D. Role of superoxide in the photochemical reduction of iron in seawater. *Geochim. Cosmochim. Acta* **2006,** *70,* 3869-3882.

214. Morel, F. M. M.; Price, N. M. The biogeochemical cycles of trace metals in the oceans. *Science* **2003,** *300,* 944-947.

215. Voelker, B. M.; Sedlak, D. L.; Zafiriou, O. C. Chemistry of superoxide radical in seawater: reactions with organic Cu complexes. *Environ. Sci. Technol.* **2000,** *34,* 1036-1042.

216. Zafiriou, O. C.; Voelker, B. M.; Sedlak, D. L. Chemistry of superoxide radical (O_2^-) in seawater: reactions with inorganic Cu complexes. *J. Phys. Chem.* **1998,** *102,* 5693-5700.

217. Petasne, R. G.; Zika, R. G. Fate of superoxide in coastal sea water. *Nature* **1987,** *325,* 516-518.

218. Micinski, E.; Ball, L. A.; Zafiriou, O. C. Photochemical oxygen activation: Superoxide radical detection and production rates in the eastern Caribbean. *J. Geophys. Res.* **1993,** *98,* 2299-2306.

219. Scully, N. M.; McQueen, D. J.; Lean, D. R. S. Hydrogen peroxide formation: The interaction of ultraviolet radiation and dissolved organic carbon in lake waters along a 43-75 ^{o}N gradient. *Limnol. Oceanogr.* **1996,** *41,* 540-548.

220. Diaz, J. M.; Hansel, C. M.; Voelker, B. M.; Mendes, C. M.; Andeer, P. F.; Zhang, T. Widespread production of extracellular superoxide by heterotrophic bacteria. *Science* **2013,** *340,* 1223-1226.

221. Hansard, S. P.; Vermilyea, A. W.; Voelker, B. M. Measurements of superoxide radical concentration and decay kinetics in the Gulf of Alaska. *Deep-Sea Res. I* **2010,** *57,* 1111-1119.

222. Goldstone, J. V.; Voelker, B. M. Chemistry of superoxide radical in seawater: CDOM associated sink of superoxide in coastal waters. *Environ. Sci. Technol.* **2000,** *34,* 1043-1048.

223. Heller, M. I.; Croot, P. M. Kinetics of superoxide reactions with dissolved organic matter in

tropical Atlantic surface waters near Cape Verde (TENATSO). *J. Geophys. Res.* **2010,** *115,* C12038, doi:10.1029/2009JC006021.

224. Wuttig, K.; Heller, M. I.; Croot, P. M. Pathways of superoxide (O_2^-) decay in the eastern tropical North Atlantic. *Environ. Sci. Technol.* **2013,** *47,* 10249-10256.

225. Garg, S.; Rose, A. L.; Waite, T. D. Photochemical production of superoxide and hydrogen peroxide from natural organic matter. *Geochim. Cosmochim. Acta* **2011,** *75,* 4310-4320.

226. Miller, G. W.; Morgan, C. A.; Kieber, D. J.; King, D. W.; Snow, J. A.; Heikes, B. G.; Mopper, K.; Kiddle, J. J. Hydrogen peroxide method intercomparision study in seawater. *Mar. Chem.* **2005,** *97,* 4-13.

227. Cooper, W. J.; Shao, C.; Lean, D. R. S.; Gordon, A. S.; Scully, F. E. J. Factors affecting the distribution of H_2O_2 in surface waters. In *Advances in Chemistry, Series;* Baker, L., Ed.; American Chemical Society, 1994; Vol. 237.

228. Garg, S.; Rose, A. L.; Waite, T. D. Production of reactive oxygen species on photolysis of dilute aqueous quinone solutions. *Photochem. Photobiol.* **2007,** *83,* 904-913.

229. Pilling, M. J.; Seakins, P. W. *Reaction Kinetics;* Oxford University Press: Oxford, UK, 1997.

230. Grebel, J. E.; Pignatello, J. J.; Song, W.; Cooper, W. J.; Mitch, W. A. Impact of halides on the photobleaching of dissolved organic matter. *Mar. Chem.* **2009,** *115,* 134-144.

231. Guerard, J. J.; Chin, Y.-P. Photodegradation of ormetoprim in aquaculture and stream-derived dissolved organic matter. *J. Ag. Food Chem.* **2012,** *60,* 9801-9806.

232. Vione, D.; Ponzo, M.; Bagnus, D.; Maurino, V.; Minero, C.; Carlotti, M. E. Comparison of different probe molecules for the quantification of hydroxyl radicals in aqueous solution. *Environ. Chem. Lett.* **2010,** *8,* 95-100.

233. Page, S. E.; Arnold, W. A.; McNeill, K. Assessing the contribution of free hydroxyl radical in organic matter-sensitized photohydroxylation reactions. *Environ. Sci. Technol.* **2011,** *45,* 2818-2825.

234. Miller, C. J.; Rose, A. L.; Waite, T. D. Hydroxyl radical production by H_2O_2-mediated oxidation of Fe(II) complexed by Suwannee River fulvic acid under circumneutral freshwater conditions. *Environ. Sci. Technol.* **2013,** *47,* 829-835.

235. Vione, D.; Falletti, G.; Maurino, V.; Minero, C.; Pelizzetti, E.; Malandrino, M.; Ajassa, R.;

Olariu, R.-I.; Arsene, C. Sources and sinks of hydroxyl radicals upon irradiation of natural water samples. *Environ. Sci. Technol.* **2006,** *40,* 3775-3781.

236. Grannas, A. M.; Martin, C. B.; Chin, Y.-P.; Platz, M. Hydroxyl radical production from irradiated Arctic dissolved organic matter. *Biogeochem.* **2006,** *78,* 51-66.

237. White, E. M.; Vaughan, P. P.; Zepp, R. G. Role of the photo-Fenton reaction in the production of hydroxyl radicals and photobleaching of colored dissolved organic matter in a coastal river of the southeastern United States. *Aquat. Sci.* **2003,** *65,* 402-414.

238. Nakatani, N.; Ueda, M.; Shindo, H.; Takeda, K.; Sakugawa, H. Contribution of the photo-Fenton reaction to hydroxyl radical formation rates in river and rain water samples. *Anal. Sci.* **2007,** *23,* 1137-1142.

239. Zhu, B.-Z.; Kalyanaraman, B.; Jiang, G.-B. Molecular mechanism for metal-independent production of hydroxyl radicals by hydrogen peroxide and halogenated quinones. *PNAS* **2007,** *104,* 17575-17578.

240. Harriman, A.; Mills, A. Photochemistry of anthraquinone-2,6-disodium sulfonate in aqueous solution. *Photochem. Photobiol.* **1981,** *33,* 619–625.

241. Gorner, H. Photoprocesses of p-benzoquinones in aqueous solution. *J. Phys. Chem.* **2003,** *107,* 11587-11595.

242. Gan, D.; Jia, M.; Vaughan, P. P.; Falvey, D. E.; Blough, N. V. Aqueous photochemistry of methyl-benzoquinone. *J. Phys. Chem. A* **2008,** *112,* 2803-2812.

243. Loeff, I.; Treinin, A.; Linschitz, H. Photochemistry of 9,10-anthraquinone-2-sulfonate in solution. 1. Intermediates and mechanism. *J. Phys. Chem.* **1983,** *87,* 2536–2544.

244. Dong, M. M.; Rosario-Ortiz, F. L. Photochemical formation of hydroxyl radical from effluent organic matter. *Environ. Sci. Technol.* **2012,** *46,* 3788-3794.

245. Xie, H.; Bélanger, S.; Demers, S.; Vincent, W. F.; Papakyriakou, T. N. Photobiogeochemical cycling of carbon monoxide in the southeastern Beaufort Sea in spring and autumn. *Limnol. Oceanogr.* **2009,** *54,* 234–249.

246. Peterson, B.; McNally, A. M.; Cory, R. M.; Thoemke, J. D.; Cotner, J. B.; McNeill, K. Spatial and temporal distribution of singlet oxygen in Lake Superior. *Environ. Sci. Technol.* **2012,** *46,* 7222–7229.

247. Pos, W. H.; Riemer, D. D.; Zika, R. G. Carbonyl sulfide (OCS) and carbon monoxide (CO)

in natural waters: evidence of a coupled production pathway. *Mar. Chem.* **1998,** *62,* 89-101.

609

610

List of Figures

Figure 1: (a) Absorption spectra for 75 mg/L Suwannee River FA at pH 7. (b) Area normalized spectra. Untreated (black line), borohydride reduced (dashed line), photobleached for 59 h with a Xe lamp (red line).

Figure 2: Fluorescence spectra for 30 mg/L Suwannee River FA: (a) & (b) Emission spectra over the excitation wavelength range 335 to 495 nm, (a) untreated, (b) borohydride reduced; (c) & (d) Excitation-emission matrix spectra, (c) untreated, (d) borohydride reduced.

Figure 3: Wavelength dependence of various quantum yields for CDOM. (a) Dissolved inorganic carbon: solid lines from equations in ref. (*154*) (Mackenzie Shelf water) and ref. (*40*) (inshore coastal waters), data points from ref. (*156*) (Satilla River CDOM). (b) Aqueous electron: Suwannee River FA (●), and Suwannee River HA (△) with power law fits to the data (*111*). (c) Hydrogen peroxide with power law fits visually delineating the maximum and minimum trends: (●) well and pond water (*138*), (△) Elizabeth River, VA (*155*). (d) Singlet oxygen with power law fits visually delineating the maximum and minimum trends: (●) Birkenes stream and Suwannee River HA (*38*), (△) aquatic FA and CDOM (*108*), (■) Black Lake HA and Lake Baldegg CDOM (*113*).

Figure 4: Model of CDOM photophysics and photochemistry. P represents an exogenous electron donor (e.g., phenol or amine contaminant).

Graphical Abstract for Table of Contents

Summary text: A critical review presenting the case for an electronic interaction model as the basis for CDOM optical and photochemical properties.

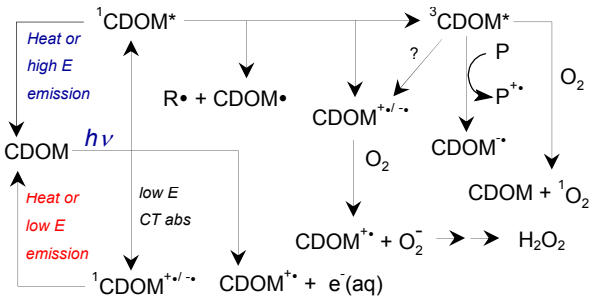

641 **Figure 1**

642

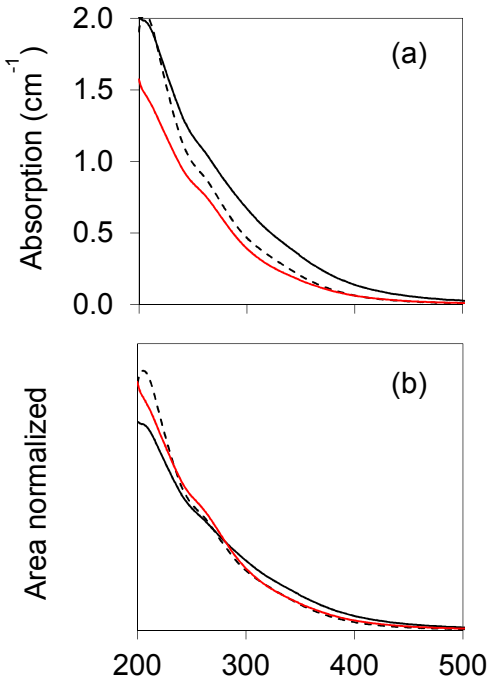

643
644
645

646 **Figure 2**

647

648

649

650

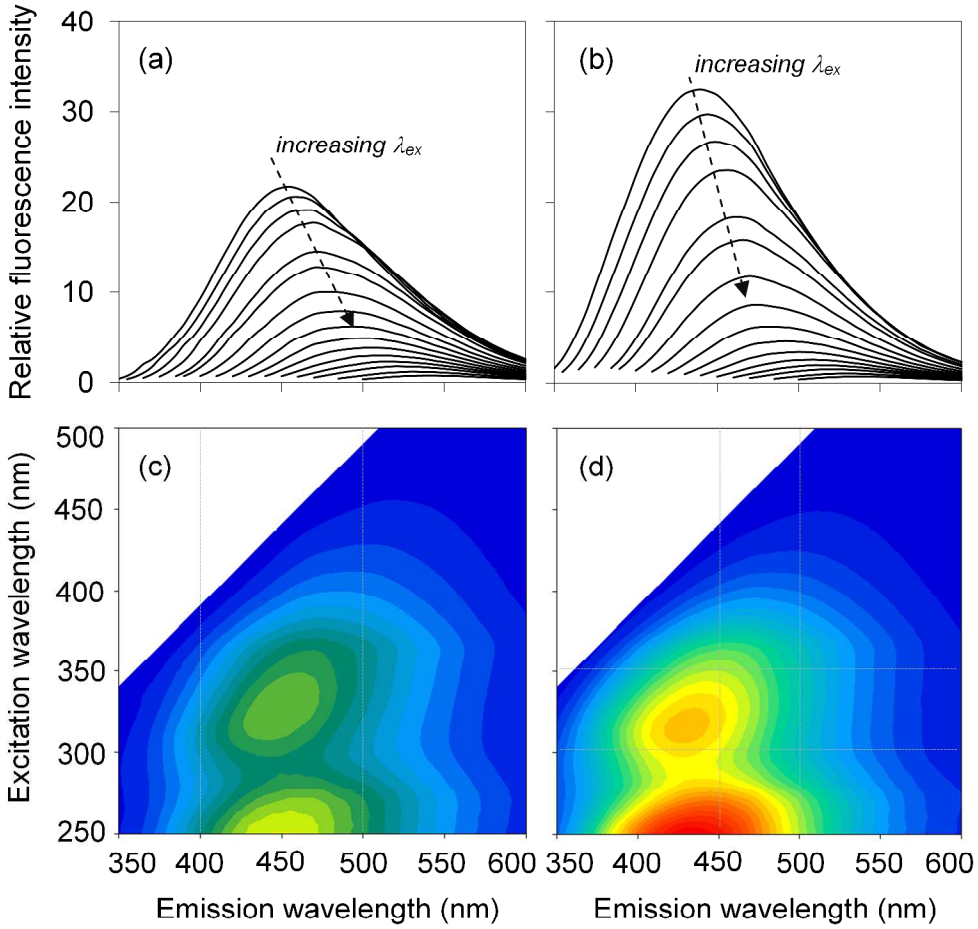

651 **Figure 3**

652

653

654

655

656

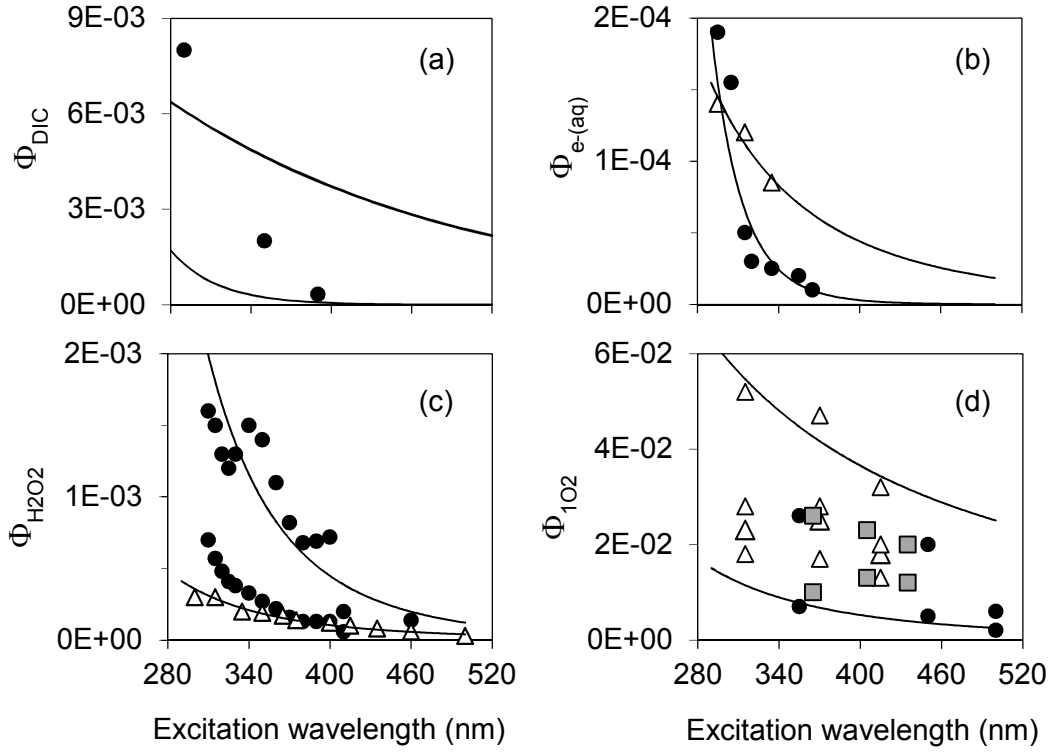

Figure 4

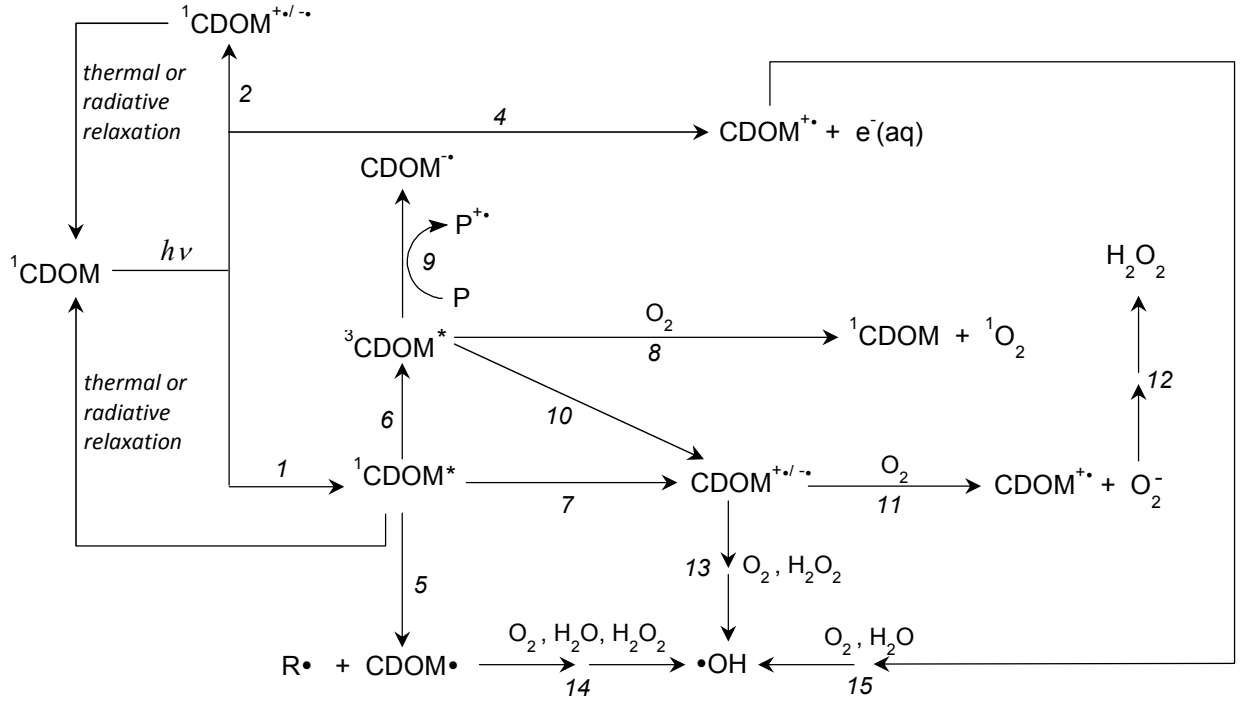
$^1CDOM^{+\bullet/-\bullet}$
thermal or radiative relaxation
2
4
$CDOM^{+\bullet}$ + $e^-(aq)$
$CDOM^{-\bullet}$
$P^{+\bullet}$
9
P
^1CDOM
$h\nu$
H_2O_2
$^3CDOM^*$
O_2
8
^1CDOM + $^1O_2$
12
thermal or radiative relaxation
6
10
1
$^1CDOM^*$
$CDOM^{+\bullet/-\bullet}$
O_2
7
11
$CDOM^{+\bullet}$ + O_2^-
13 O_2, H_2O_2
5
O_2, H_2O, H_2O_2
O_2, H_2O
R• + CDOM•
•OH
14
15